Wandering breathers and self-trapping in weakly coupled nonlinear chains: Classical counterpart of macroscopic tunneling quantum dynamics

Yu. A. Kosevich,* L. I. Manevitch,† and A. V. Savin‡
Semenov Institute of Chemical Physics, Russian Academy of Sciences, ul. Kosygina 4, 119991 Moscow, Russia
(Received 2 August 2006; revised manuscript received 25 December 2007; published 14 April 2008)

We present analytical and numerical studies of the phase-coherent dynamics of intrinsically localized excitations (breathers) in a system of two weakly coupled nonlinear oscillator chains. We show that there are two qualitatively different dynamical regimes of the coupled breathers, either immovable or slowly moving: the periodic transverse translation (wandering) of the low-amplitude breather between the chains and the one-chain-localization of the high-amplitude breather. These two modes of coupled nonlinear excitations, which involve a large number of anharmonic oscillators, can be mapped onto two solutions of a single pendulum equation, detached by a separatrix mode. We also show that these two regimes of coupled phase-coherent breathers are similar and are described by a similar pair of equations to the two regimes in the nonlinear tunneling dynamics of two weakly linked interacting (nonideal) Bose-Einstein condensates. On the basis of this profound analogy, we predict a tunneling mode of two weakly coupled Bose-Einstein condensates in which their relative phase oscillates around $\frac{\pi}{2}$ mod π. We also show that the magnitude of the static displacements of the coupled chains with nonlinear localized excitation, induced by the cubic term in the intrachain anharmonic potential, scales approximately as the total vibrational energy of the excitation, either a one- or two-chain one, and does not depend on the interchain coupling. This feature is also valid for a narrow stripe of several parallel-coupled nonlinear chains. We also study two-chain breathers which can be considered as bound states of discrete breathers, with different symmetry and center locations in the coupled chains, and bifurcation of the antiphase two-chain breather into the one-chain one. Bound states of two breathers with different commensurate frequencies are found in the two-chain system. Merging of two breathers with different frequencies into one breather in two coupled chains is observed. Wandering of the low-amplitude breather in a system of several, up to five, coupled nonlinear chains is studied, and the dependence of the wandering period on the number of chains is analytically estimated and compared with numerical results. The delocalizing transition of a one-dimensional (1D) breather in the 2D system of a large number of parallel-coupled nonlinear oscillator chains is described, in which the breather, initially excited in a given chain, abruptly spreads its vibrational energy in the whole 2D system upon decreasing the breather frequency or amplitude below the threshold one. The threshold breather frequency is above the cutoff phonon frequency in the 2D system, and the threshold breather amplitude scales as the square root of the interchain coupling constant. The delocalizing transition of the discrete vibrational breather in 2D and 3D systems of parallel-coupled nonlinear oscillator chains has an analogy with the delocalizing transition for Bose-Einstein condensates in 2D and 3D optical lattices.

DOI: 10.1103/PhysRevE.77.046603 PACS number(s): 05.45.Yv, 74.81.Fa, 03.75.Lm, 74.50.+r

I. INTRODUCTION

Nonlinear excitations (solitons, kink-solitons, intrinsically localized modes, and breathers) can be created most easily in low-dimensional [one-dimensional (1D) and quasi-1D] systems [1–10]. Recent experiments have demonstrated the existence of intrinsically localized modes and breathers in various systems such as 2D and 3D arrays of nonlinear optical waveguides [11,12], low-dimensional crystals [13], antiferromagnetic materials [14], Josephson junction arrays [15,16], photonic structures and micromechanical systems [17], protein α-helices [18], and α-uranium [19]. Slowly moving breathers and supersonic kink-solitons were also described in 1D nonlinear chains [6,7,20–23], DNA macromolecules [24], and quasi-1D polymer crystals [25,26].

One-dimensional arrays of magnetic or optical microtraps for Bose-Einstein condensates (BECs) of ultracold quantum gases with tunneling coupling provide a new field for studies of the coherent nonlinear dynamics in low-dimensional systems [27,28]. In the mean-field theory, the tunneling coupling between two interacting BECs is similar to the linear coupling between two nonlinear optical waveguides [29] or between two chains of anharmonic oscillators (nonlinear phononic waveguides) [30]. Here we show that the *phase-coherent* dynamics of macroscopic ensembles of classical particles (weakly localized breathers) in two weakly linked nonlinear oscillator chains has a profound analogy and is described by a similar, in every respect, pair of equations to the tunneling quantum dynamics of two weakly linked interacting (nonideal) BECs in a macroscopic double-well potential (single-bosonic Josephson junction) [31]. The exchange of energy and excitations between the coupled classical oscillator chains takes on the role which the exchange of atoms via quantum tunneling plays in the case of coupled BECs. Therefore such phase-coherent energy and excitation ex-

*yukosevich@yahoo.com
†lmanev@center.chph.ras.ru
‡asavin@center.chph.ras.ru

change can be considered as a classical counterpart of macroscopic tunneling quantum dynamics.

We show that there are two qualitatively different dynamical regimes of the coupled breathers: the oscillatory exchange of the low-amplitude breather between the chains (*wandering breather*) and one-chain-localization (nonlinear self-trapping) of the high-amplitude breather. These two regimes, which are detached by a separatrix mode with a zero rate of energy and excitation exchange, are analogous to the two regimes in the nonlinear dynamics of macroscopic interacting condensates in a single-bosonic Josephson junction [31]. Essentially, the phase-coherent dynamics of the coupled classical breathers is described by a pair of equations, which coincides with the pair of coupled mean-field equations describing coherent atomic tunneling in a single-bosonic tunnel junction [32,33]. The predicted evolution of the relative phase of two weakly coupled coherent breathers in both dynamical regimes is also analogous to the evolution of the relative quantum mechanical phase between two weakly coupled macroscopic condensates, which was directly measured in a single-bosonic Josephson junction by means of interference [31]. Moreover, the predicted separatrix in the excitation exchange between macroscopic ensembles of phase-coherent particles (weakly localized breathers) in coupled oscillator chains with "repulsive" nonlinearity, which is determined by the ratio of the intrachain nonlinearity (intrachain interaction) and the interchain coupling, can be considered as a classical nonlinear dynamical model of the reversible interaction-induced superfluid–Mott-insulator quantum phase transition, observed in BECs with repulsive interatomic interaction in a lattice with tunneling intersite coupling [34]. All these results bring to light a striking similarity, in both display and evolution equations, between the classical phase-coherent excitation exchange and macroscopic tunneling quantum dynamics which can motivate new predictions and experiments in both fields. On the basis of this profound analogy, we predict a tunneling regime of two weakly coupled BECs in which their relative phase oscillates around $\frac{\pi}{2}$ mod π, which can be observed by means of interference. This regime is different from the regime of Josephson plasma oscillations, already realized in experiments [31], in which the relative phase of two weakly linked BECs oscillates (or fluctuates [35]) around zero.

We also show that the magnitude of the static displacements of the coupled chains with nonlinear localized excitation, caused by the cubic term in the intrachain anharmonic potential, scales approximately as the total vibration energy of the excitation, either the one- or two-chain one, and does not depend on the interchain coupling. This feature is also valid for a narrow stripe of several parallel-coupled nonlinear chains. We also study two-chain breathers which can be considered as bound states of discrete breathers with different symmetry and center locations in the coupled chains, and bifurcation of the antiphase two-chain breather into the one-chain one. Bound states of two breathers with different commensurate frequencies are also found in the two-chain system. Merging of two breathers with different frequencies into one breather in two coupled chains is described. Periodic transverse translation (wandering) of a low-amplitude breather in a system of several, up to five, coupled nonlinear chains is observed, and the dependence of the wandering period on the number of chains is analytically estimated and compared with numerical results. The delocalizing transition of a 1D breather in a 2D system of a large number of parallel-coupled nonlinear oscillator chains is described, in which the breather, initially excited in a given 1D chain, abruptly spreads its vibrational energy in the whole 2D system upon decreasing the breather frequency or amplitude below the threshold one. The threshold breather frequency is above the cutoff phonon frequency in the 2D system, the threshold breather amplitude scales as the square root of the interchain coupling constant, and the breather vibrational energy is localized mainly in one chain at the delocalization threshold. A similar delocalizing transition for the 1D breather should occur also in a 3D array of parallel-coupled nonlinear chains. The delocalizing transition of a discrete breather in 2D and 3D systems of coupled nonlinear oscillator chains has an analogy with the delocalizing transition for polarons in 2D and 3D lattices [36] and for Bose-Einstein condensates in 2D and 3D optical lattices [37].

The paper is organized as follows. In the next section, Sec. II, we describe our model and the analytical predictions, derived on the basis of this model. In Sec. III we describe our numerical simulations and comparison with the analytical predictions, which include simulation of the dynamics of discrete breathers in two weakly coupled chains (Sec. III A), simulation of a wandering breather in two weakly coupled chains (Sec. III B), and simulation of breathers in a system of $M>2$ parallel weakly coupled anharmonic chains (Sec. III C). In Sec. IV we give a summary of the main results of this paper.

II. MODEL AND ANALYTICAL PREDICTIONS

We consider two linearly coupled nonlinear oscillator chains (with unit lattice period). We model the chains with the Fermi-Pasta-Ulam (FPU) Hamiltonian, which is one of the most simple and universal models of nonlinear lattices and which can be applied to a diverse range of physical problems [38]:

$$H=\sum_{i=1}^{2}\sum_{n}\left[\frac{1}{2}p_n^{(i)2}+\frac{1}{2}l^{(i)}(u_{n+1}^{(i)}-u_n^{(i)})^2+\frac{1}{3}\alpha^{(i)}(u_{n+1}^{(i)}-u_n^{(i)})^3+\frac{1}{4}\beta^{(i)}(u_{n+1}^{(i)}-u_n^{(i)})^4+\frac{1}{2}C(u_n^{(i)}-u_n^{(3-i)})^2\right]. \quad (1)$$

Here $u_n^{(i)}$ is displacement of the nth particle from its equilibrium position in the ith chain, $p_n^{(i)}=\dot{u}_n^{(i)}$ is the particle momentum, $l^{(i)}$, $\alpha^{(i)}$, and $\beta^{(i)}$ are the intrachain linear and nonlinear force constants, and C describes the linear interchain coupling. We assume that the coupling is weak, $C\ll l^{(i)}$, and do not include the nonlinear interchain interaction. The β-FPU Hamiltonian (1) (with $\alpha^{(i)}=0$) describes, in particular, purely transverse particle motion [6]. The torsion dynamics of the DNA double helix can also be approximated by the β-FPU Hamiltonian (1) [24]. On the other hand, weakly coupled nonlinear molecular chains in polymers are characterized by the asymmetric intrachain anharmonic potential, with nonzero $\alpha^{(i)}$ [25,26].

The Hamiltonian (1) generates the following equations of motion, $i=1,2$:

$$\ddot{u}_n^{(i)} = l^{(i)}(u_{n+1}^{(i)} + u_{n-1}^{(i)} - 2u_{n+1}^{(i)}) + \alpha^{(i)}[(u_{n+1}^{(i)} - u_n^{(i)})^2 - (u_{n-1}^{(i)} - u_n^{(i)})^2] + \beta^{(i)}[(u_{n+1}^{(i)} - u_n^{(i)})^3 + (u_{n-1}^{(i)} - u_n^{(i)})^3] + C(u_n^{(3-i)} - u_n^{(i)}). \quad (2)$$

Below we consider two chains with identical anharmonic force constants when $\alpha^{(1)}=\alpha^{(2)}\equiv\alpha$ and $\beta^{(1)}=\beta^{(2)}\equiv\beta$. We are interested in the high-frequency and therefore short-wavelength dynamics of the coupled chains when the displacements of the nearest-neighbor particles are mainly antiphase. For this case we can introduce continuous envelope functions for the particle displacements in the chains, $f_n^{(i)}=u_n^{(i)}(-1)^n$ and $f_n^{(i)}\equiv f(x)_i$. These envelope functions $f(x)_i$ are supposed to be slowly varying on the interatomic scale in both chains, $\partial f_i/\partial x \ll 1$, which allows us to write the corresponding partial differential equations for these functions; see, e.g., Refs. [2,6,7,21]. To obtain nonlinear envelope-function equations for the coupled chains with asymmetric interparticle potential, one needs to consider separately the dynamics of the *relative*, $v_n^{(i)}=u_{n+1}^{(i)}-u_n^{(i)}$, and *total*, $w_n^{(i)}=u_{n+1}^{(i)}+u_n^{(i)}$, displacements of the nearest-neighbor particles; cf. Ref. [2]. Equations for $v_n^{(i)}$ and $w_n^{(i)}$ can be obtained from Eqs. (2) and look as follows:

$$\ddot{v}_n^{(i)} = l^{(i)}(v_{n+1}^{(i)} + v_{n-1}^{(i)} - 2v_{n+1}^{(i)}) + \alpha[v_{n+1}^{(i)2} + v_{n-1}^{(i)2} - 2v_n^{(i)2}] + \beta[v_{n+1}^{(i)3} + v_{n-1}^{(i)3} - 2v_n^{(i)3}] + C(v_n^{(3-i)} - v_n^{(i)}), \quad (3)$$

$$\ddot{w}_n^{(i)} = l^{(i)}(w_{n+1}^{(i)} + w_{n-1}^{(i)} - 2w_{n+1}^{(i)}) + \alpha[v_{n+1}^{(i)2} - v_{n-1}^{(i)2}] + \beta[v_{n+1}^{(i)3} - v_{n-1}^{(i)3}] + C(w_n^{(3-i)} - w_n^{(i)}). \quad (4)$$

Introducing the continuous relative and total displacements $v_n^{(i)}\equiv v(x)_i$ and $w_n^{(i)}\equiv w(x)_i$ and making in Eqs. (3) and (4) expansions of the differences $u_{n\pm1}^{(i)}-u_n^{(i)}$ and $w_{n\pm1}^{(i)}-w_n^{(i)}$ up to second order, we get the following partial differential equations for $v(x,t)_i$ and $w(x,t)_i$:

$$\ddot{v}_i = -l^{(i)}\frac{\partial^2 v_i}{\partial x^2} - 4l^{(i)}v_i - 4\frac{\partial w_i}{\partial x}(\alpha v_i + \beta v_i^2) - 4\beta v_i^3 + C(v_{3-i} - v_i), \quad (5)$$

$$\ddot{w}_i = l^{(i)}\frac{\partial^2 w_i}{\partial x^2} + 2\alpha\frac{\partial v_i^2}{\partial x} + 2\beta\frac{\partial v_i^3}{\partial x} + C(w_{3-i} - w_i). \quad (6)$$

The main small parameters, which will allow us to find asymptotic solutions of these equations, are the amplitudes of the displacements $u_n^{(i)}$ of the coupled oscillations and hence their envelopes $f(x,t)_i$. As follows from Eqs. (6), in the chains with asymmetric interparticle potential (with finite α) the total displacements w_i of the nearest neighbors are weakly coupled (via anharmonic interaction) with relative displacements v_i and are in general small in comparison with them, $w_i \ll v_i$ [see Eqs. (9)–(11) below]. In such chains, the asymmetric potential induces both the static (zeroth-harmonic) and second-harmonic terms in the total displacements of the nearest-neighbor particles, but the latter terms are smaller than the former ones in the small-amplitude limit; cf. Ref. [2].

Now we analyze the static displacements $w_{0i}(x)$ of two *identical* weakly coupled chains with $l^{(1)}=l^{(2)}=1$. In order to minimize the static elastic energy, the static displacements of the chains should be equal *at both infinities*: $w_{01}(x)=w_{02}(x)$ for $x\to-\infty$ and $x\to+\infty$. To find $w_{0i}(x)$, we take the sum and difference of Eqs. (6) for the two chains to obtain the following equations:

$$\ddot{w}_1 + \ddot{w}_2 = \frac{\partial^2(w_1+w_2)}{\partial x^2} + 2\alpha\frac{\partial(v_1^2+v_2^2)}{\partial x} + 2\beta\frac{\partial(v_1^3+v_2^3)}{\partial x}, \quad (7)$$

$$\ddot{w}_1 - \ddot{w}_2 = \frac{\partial^2(w_1-w_2)}{\partial x^2} - 2C(w_1-w_2) + 2\alpha\frac{\partial(v_1^2-v_2^2)}{\partial x} + 2\beta\frac{\partial(v_1^3-v_2^3)}{\partial x}. \quad (8)$$

Omitting the time-derivative terms, we get from Eq. (7) the following expression for the static center-of-mass displacement of the two chains:

$$w_0^{(\mathrm{c.m.})}(x) = \frac{w_{01}(x)+w_{02}(x)}{2} = -\alpha\int_{-\infty}^{x}\langle v_1^2+v_2^2\rangle dx', \quad (9)$$

where the angular brackets denote the time averaging. The nonlinear term, proportional to $\beta\langle v_1^3+v_2^3\rangle$ [cf. Eq. (7)], is averaged out in Eq. (9) because of the third power of $v^{(i)}$. At both infinities, the displacement $w_0^{(\mathrm{c.m.})}(x)$ coincides with equal static displacements of the coupled chains, $w_0^{(\mathrm{c.m.})}(\pm\infty)=w_0^{(1)}(\pm\infty)=w_0^{(2)}(\pm\infty)$. It is assumed in Eq. (9) that $w_0^{(\mathrm{c.m.})}(-\infty)=0$, $v^{(i)}(-\infty)=0$, and $\frac{\partial w_0^{(\mathrm{c.m.})}}{\partial x}(-\infty)=0$, $i=1,2$. Therefore the static displacements of the both coupled chains $w_0(x)^{(i)}$ have in general the form of the *kinklike* pattern with equal center-of-mass displacement difference $\Delta w_0^{(\mathrm{c.m.})}=w_0^{(\mathrm{c.m.})}(+\infty)-w_0^{(\mathrm{c.m.})}(-\infty)=w_0^{(\mathrm{c.m.})}(+\infty)$. The kinklike static displacement pattern of an intrinsically localized mode (breather) in a *single* α-β-FPU chain was studied in Refs. [2,39–41].

The term in angular brackets on the right-hand side of Eq. (9) coincides with the total vibration energy of two coupled chains [in the low-amplitude limit when the energy is governed mainly by the quadratic terms in Hamiltonian (1)]. Therefore the magnitude of the center-of-mass displacement of the coupled chains with asymmetric anharmonic potential scales approximately as the *total vibrational energy* of the nonlinear localized excitation, the one- or the two-chain breather in two coupled chains: $w_0^{(\mathrm{c.m.})}=-\alpha\int_{-\infty}^{+\infty}\langle v_1^2+v_2^2\rangle dx'$. Equations (7) and (9) also show that static *strain* of the chains, given by the displacement derivative, is determined by the *local density* of the total vibrational energy of the nonlinear localized excitation: $\partial w_0^{(\mathrm{c.m.})}(x)/\partial x=-\alpha\langle v_1^2+v_2^2\rangle(x)$. These conclusions are confirmed by our numerical simulations; see Figs. 2(c) and 2(d) below.

These conclusions can be easily generalized to the system of $M>2$ parallel-coupled nonlinear chains, see also Sec. III C below. In this case only the last term in Eqs. (5) and (6),

describing the interchain coupling, will be modified [cf. Eq. (62) below]. In a narrow stripe of chains, when the number of particles, N, in each chain greatly exceeds the number of chains, $N \gg M$, the static center-of-mass displacement in the multichain system will have the form

$$w_0^{(\mathrm{c.m.})}(x) = \frac{1}{M}\sum_{m=1}^{M} w_{0m}(x) = -\frac{2\alpha}{M}\int_{-\infty}^{x}\left\langle \sum_{m=1}^{M} v_m^2 \right\rangle dx', \tag{10}$$

where $v_m(x)$ and $w_{0m}(x)$ are, respectively, the relative and static total nearest-neighbor displacements in the mth chain. It is assumed in Eq. (10) that $w_0^{(\mathrm{c.m.})}(-\infty)=0$, $v_m(-\infty)=0$, and $\frac{\partial w_0^{(\mathrm{c.m.})}}{\partial x}(-\infty)=0$. As follows from Eq. (10), the lattice displacement $w_0^{(\mathrm{c.m.})}(x)$ and the corresponding lattice strain $\partial w_0^{(\mathrm{c.m.})}/\partial x$ in the multichain system depend on the number of the oscillating chains and on their vibrational energies. Importantly, the magnitudes of the static lattice displacements and of the strain in a system of coupled chains, Eqs. (9) and (10), do not depend on the strength of the interchain coupling, which is related to the long-range action of the static elastic fields.

The magnitudes of the static displacements in the central region of the kinks in the two chains are different in general and can be found with the help of Eq. (8) and the above requirements for the magnitudes of $w_0(x)^{(i)}$ at the infinities. Omitting the time-derivative terms, we get from Eq. (8) the following solution for the difference of static displacements of the two coupled chains:

$$\begin{aligned}\Delta w_0(x) &\equiv w_{01}(x) - w_{02}(x) \\ &= \frac{1}{4}\sqrt{\frac{2}{C}}\left\langle \int_{-\infty}^{x} \sinh[(s-x)\sqrt{2C}]A(s)ds \right. \\ &\quad + \int_{x}^{\infty} \sinh[(x-s)\sqrt{2C}]A(s)ds \\ &\quad - \int_{-\infty}^{-x} \sinh[(s+x)\sqrt{2C}]A(s)ds \\ &\quad \left. + \int_{-x}^{\infty} \sinh[(s+x)\sqrt{2C}]A(s)ds \right\rangle, \end{aligned} \tag{11}$$

where $A(s)=\alpha\,\partial[v_1^2(s)-v_2^2(s)]/\partial s$. Taking into account that $v_i^2(x)$ is a symmetric function with respect to the breather center $x=0$ [see Eqs. (19) and (20) below], Eq. (11) gives us that $\Delta w_0(x)=-\Delta w_0(-x)$ and therefore $\Delta w_0(x)$ is zero both at $x=0$ and at both infinities. [As follows from Eq. (11), the difference of the static displacements of the coupled chains $\Delta w_0(x)$ depends in general on the coupling constant C, in contrast to the static center-of-mass displacement $w_0^{(\mathrm{c.m.})}(x)$, Eq. (9).] As follows in turn from Eqs. (6), the second-harmonic terms in the total displacements $w(x)^i$ in the chains have smallness of the third order in $v(x)^{(i)}$ because of the smallness of the spatial derivative $\partial v^{(i)2}/\partial x \sim \lambda_i v^{(i)2} \sim v^{(i)3}$; see Eqs. (19), (20), and (23) below. This allows us to neglect in the following analysis of breather dynamics in coupled chains both the difference of static displacements of the chains $\Delta w_0(x)$ and the second-harmonic terms in the total displacements $w(x)^i$ in comparison with the static center-of-mass displacement $w_0^{(\mathrm{c.m.})}(x)$.

Taking into account that $v(x)_i=2f(x)_i$, we get from Eqs. (5), (7), and (9) the following coupled nonlinear partial differential equations for the real envelope functions $f(x)_i$, $i=1,2$:

$$\ddot{f}_i + \omega_{mi}^2 f_i + \frac{\partial^2 f_i}{\partial x^2} + 16\beta f_i^3 - 16\alpha^2\langle f_1^2 + f_2^2\rangle f_i - C f_{3-i} = 0, \tag{12}$$

where $\omega_{mi}=\sqrt{4l^{(i)}+C}$ is the characteristic frequency slightly above the maximal phonon frequency in the ith isolated chain. These self-consistent equations describe the dynamical relative lattice displacements $v_i(x)$, while the static lattice displacements $w_{0i}(x)$ can be obtained with the use of Eqs. (9) and (11). It is worth mentioning that collective static deformation of the coupled chains, induced by the asymmetric intrachain anharmonic potential, makes the coupled envelope-function equations (12) *nonlocal* in general, via the term proportional to $-\alpha^2$.

In order to deal with the amplitude and phase of the coupled nonlinear excitations, it is useful to introduce complex wave fields $\Psi(x,t)_i$ for each chain (see, e.g., Ref. [21]):

$$f(x,t)_i = \frac{1}{2}[\Psi(x,t)_i + \Psi(x,t)_i^*]. \tag{13}$$

Then in resonance approximation we get from Eqs. (12) and (13) the following coupled equations for $\Psi(x,t)_i$, $i=1,2$:

$$\begin{aligned}&\frac{1}{2}\left(\frac{\partial^2\Psi_i}{\partial t^2} + \frac{\partial^2\Psi_i}{\partial x^2} + \omega_{mi}^2\Psi_i\right) + 6\beta|\Psi_i|^2\Psi_i \\ &\quad - 8\alpha^2\langle|\Psi_1|^2 + |\Psi_2|^2\rangle\Psi_i - \frac{1}{2}C\Psi_{3-i} = 0 \end{aligned} \tag{14}$$

(and complex-conjugated equations for Ψ_i^*). This approximation, in which we neglect the higher harmonics, is valid for the dispersive system under consideration due to the weakness of the nonresonant interaction between the mode with fundamental frequency and its third harmonic; cf. Ref. [21].

Using Eqs. (14) in the assumption that the shift of the wandering breather frequency, caused by nonlinearity, weak interchain coupling, and slow breather motion along the chains, is relatively small, one can readily ascertain the existence in general of the following three integrals of motion:

$$N_b = \int [|\Psi_1|^2 + |\Psi_2|^2]dx, \tag{15}$$

$$\begin{aligned}E_b = \int \left[\sum_{i=1}^{2} \left(3\beta|\Psi_i|^4 - 8\alpha^2\langle|\Psi_1|^2 + |\Psi_2|^2\rangle|\Psi_i|^2 \right.\right. \\ \left.\left. - \frac{1}{2}\left|\frac{\partial\Psi_i}{\partial x}\right|^2 \right) - \frac{1}{2}C(\Psi_1\Psi_2^* + \Psi_2\Psi_1^*) \right] dx, \end{aligned} \tag{16}$$

$$P_{bx} = -\frac{i}{2}\int \sum_{i=1}^{2}\left[\Psi_i \frac{\partial \Psi_i^*}{\partial x} - \Psi_i^* \frac{\partial \Psi_i}{\partial x}\right] dx, \tag{17}$$

which play the role of the breather total number of excitations, total energy, and total momentum along the chain axis, respectively; cf. [21]. The existence of these integrals of motion demonstrates that the exchange of energy and momentum between two nonlinear systems (1) is a coherent phenomenon, which depends in general on the initial excitation conditions.

It is also useful to define partial numbers of excitations,

$$N_i = \int |\Psi_i|^2 dx, \quad i = 1,2,$$

when $\dot{N}_i + J_i = 0$, where

$$J_i = -J_{3-i} = \frac{iC}{2\omega}\int [\Psi_i \Psi_{3-i}^* - \Psi_i^* \Psi_{3-i}] dx \tag{18}$$

is a total interchain flux of excitations, which conserves the total number of them, $\dot{N}_b = 0$, where $N_b = N_1 + N_2$, and ω is the frequency of the wandering breather; see Eqs. (19), (20), and (22) below.

To describe with the help of Eqs. (14) an immovable or slowly moving breather, wandering between two weakly coupled nonlinear chains with positive (repulsive) anharmonic force constant β, we assume the following form for the complex fields Ψ_1 and Ψ_2:

$$\Psi_1 = \Psi_{\max} \frac{\exp[i(kx - \omega t)]}{\cosh[\lambda_1 (x - Vt)]} \cos\Theta \exp\left(-\frac{i}{2}\Phi\right), \tag{19}$$

$$\Psi_2 = \Psi_{\max} \frac{\exp[i(kx - \omega t)]}{\cosh[\lambda_2 (x - Vt)]} \sin\Theta \exp\left(\frac{i}{2}\Phi\right), \tag{20}$$

where ω, $V \ll 1$, and $k \ll 1$ are, respectively, the frequency, slow velocity, and small wave number related to the moving breather, $\lambda_{1,2} \ll 1$ are real parameters describing the inverse localization lengths of the breathers; and $\Phi = \Phi(t - kx/\omega)$ stands for the relative phase of the coupled chains, while the parameter $\Theta = \Theta(t - kx/\omega)$ describes the "relative population" of the two chains, $z = (n_1 - n_2)/(n_1 + n_2) = \cos 2\Theta$, where $n_i = |\Psi_i|^2$ is the local density of excitations in the ith chain and $\langle |\Psi_1|^2 + |\Psi_2|^2 \rangle = \Psi_{\max}^2$ in Eq. (14). The parameters Θ and Φ determine also the interchain flux of excitations [cf. Eq. (18)]:

$$J_1 = -J_2 = \frac{C\Psi_{\max}^2}{2\omega}\int \frac{\sin 2\Theta \sin\Phi}{\cosh[\kappa_1 (x - Vt)]\cosh[\kappa_2 (x - Vt)]} dx. \tag{21}$$

Using Eqs. (14), (19), and (20), after some algebra we obtain dispersion equations for the introduced parameters,

$$\omega^2 = \frac{1}{2}(\omega_{m1}^2 + \omega_{m2}^2) + (3\beta - 8\alpha^2)\Psi_{\max}^2 - k^2 - C\frac{\cos\Phi}{\sin(2\Theta)}, \tag{22}$$

$$\lambda_1^2 = (6\beta\cos^2\Theta - 8\alpha^2)\Psi_{\max}^2, \quad \lambda_2^2 = (6\beta\sin^2\Theta - 8\alpha^2)\Psi_{\max}^2, \tag{23}$$

$$V = \frac{\partial\omega}{\partial k}, \tag{24}$$

and evolution equations for Φ and Θ:

$$\dot{\Phi} = \frac{1}{2\omega}(\omega_{m1}^2 - \omega_{m2}^2) + \frac{3\beta\Psi_{\max}^2}{\omega}\cos(2\Theta) + \frac{C}{\omega}\cos\Phi\cot(2\Theta), \tag{25}$$

$$\dot{\Theta} = \frac{C}{2\omega}\sin\Phi. \tag{26}$$

In the derivation of Eqs. (25) and (26), it was assumed explicitly that the ratio $\frac{\cosh[\lambda_1(x-Vt)]}{\cosh[\lambda_2(x-Vt)]}$ is equal to 1. The latter is valid for small-amplitude breathers with long localization lengths, $\lambda_{1,2} \ll 1$. In this case the above assumption, which is exact for the central region of the breathers, $x - Vt \approx 0$, will be (approximately) valid for a large number of particles, which form weakly localized wandering breathers in weakly coupled nonlinear chains. It is also assumed in the approximation considered that the shifts of the breather frequency ω, Eq. (22), caused by the weak interchain coupling C, nonlinearity $(3\beta - 8\alpha^2)\Psi_{\max}^2$, and slow breather motion along the chains k^2, as well as the characteristic frequency difference $|\omega_{m1} - \omega_{m2}|/\omega$, are all relatively small. It is worth mentioning that the parameter $-8\alpha^2\Psi_{\max}^2$ determines the shift of the breather frequency ω and inverse localization lengths $\lambda_{1,2}$ [see Eqs. (22) and (23)], but does not enter the evolution equations (25) and (26) for Θ and Φ. Equations similar to Eqs. (25) and (26) were probably derived for the first time in Ref. [42] for the description of energy exchange between two weakly coupled classical anharmonic oscillators (with $\omega_{m1} = \omega_{m2}$ and $\alpha = 0$). Later, similar equations were used for the description of the power exchange between two weakly coupled nonlinear optical waveguides [43] and of the dynamics of coupled nonlinear oscillators [44].

Equations (25) and (26) can be written in an equivalent form for the relative phase Φ and population imbalance z, when $z = \cos 2\Theta$ and $\sqrt{1 - z^2} = \sin 2\Theta$:

$$\dot{\Phi} = \omega_{m1} - \omega_{m2} + \frac{3\beta\Psi_{\max}^2}{\omega}z + \frac{C}{\omega}\frac{z}{\sqrt{1 - z^2}}\cos\Phi, \tag{27}$$

$$\dot{z} = -\frac{C}{\omega}\sqrt{1 - z^2}\sin\Phi. \tag{28}$$

Here the variables Φ and z are canonically conjugate,

$$\dot{\Phi} = \frac{\partial H_{eff}}{\partial z}, \quad \dot{z} = -\frac{\partial H_{eff}}{\partial \Phi}, \tag{29}$$

with the following effective Hamiltonian (which has the dimension of frequency):

$$H_{eff} = \frac{3\beta\Psi_{\max}^2}{2\omega} z^2 - \frac{C}{\omega}\sqrt{1-z^2}\cos\Phi + z(\omega_{m1} - \omega_{m2}). \tag{30}$$

The very same equations (27) and (28) for Φ and z, which are equivalent to Eqs. (25) and (26) for Φ and Θ, were obtained in Refs. [32,33] in the mean-field theory of tunneling dynamics of two weakly coupled interacting (nonideal) Bose-Einstein condensates, which were later used in the analysis of the experimental realization of a single-bosonic Josephson junction [31]. Therefore the generic evolution equations (27) and (28) (being written in corresponding units) for the dynamics of two coupled phase-coherent breathers or tunneling dynamics of two coupled interacting BECs do not explicitly depend on the "source" equations: Eqs. (14) for coupled oscillator chains or mean-field Gross-Pitaevskii equations for coupled interacting BECs [32,33]. In our case, Eqs. (27) and (28) describe the exchange of lattice excitations between the chains rather than atomic tunneling. One can therefore consider such an excitation exchange as a classical counterpart of macroscopic tunneling quantum dynamics. Some other equivalent forms of the effective Hamiltonian (30) were also discussed in Refs. [45,46].

It is noteworthy that equations, similar to Eqs. (25) and (26), describe the dynamics of two weakly coupled nonlinear oscillators (with different harmonic eigenfrequencies ω_{m1} and ω_{m2}) [44,47]. Therefore wandering breathers can be considered as weakly coupled phase-coherent nonlinear *macroscopic oscillators*.

Equations (25) and (26) can be solved analytically for the given initial conditions with the use of the variational method. For two *identical* chains, with $\omega_{m1}=\omega_{m2}\equiv\omega_m$, we assume that the solution of Eq. (26) has the following form:

$$\cos\Phi = A(t)/\sin(2\Theta), \tag{31}$$

where $A=0$ for $\sin(2\Theta)=0$. Using this ansatz, we get from Eqs. (25) and (26) that

$$\dot{A} = -6\frac{\beta\Psi_{\max}^2}{C}\sin(2\Theta)\cos(2\Theta)\dot{\Theta}. \tag{32}$$

For the aforementioned initial condition, when $A=0$ for $\sin(2\Theta)=0$, from Eq. (32) we find

$$A = -\frac{3\beta\Psi_{\max}^2}{2C}\sin^2(2\Theta), \tag{33}$$

$$\cos\Phi = -\frac{3\beta\Psi_{\max}^2}{2C}\sin(2\Theta) = -\frac{3\beta\Psi_{\max}^2}{2C}\sqrt{1-z^2}, \tag{34}$$

which corresponds to $\Phi=\frac{\pi}{2}$ mod π for $\sin(2\Theta)=0$. This exact solution of Eqs. (25)–(28), conserves the effective Hamiltonian (30): $H_{eff}=\frac{3\beta\Psi_{\max}^2}{2\omega}$. The important feature of this solution is that the relative phase Φ is *self-locked* to the value $\frac{\pi}{2}$ mod π by the total population imbalance $|z|=1$ of the two coupled chains.

The phase portrait of Eq. (34) in the Φ-z plane is given by

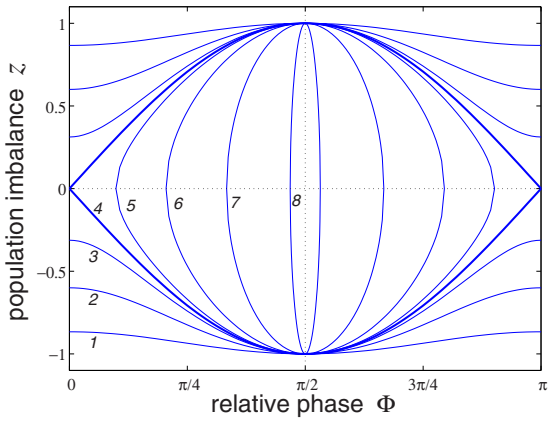

FIG. 1. (Color online) Phase portrait of a wandering breather in two weakly coupled nonlinear chains or two weakly linked BECs in a symmetric double-well potential with the initial conditions $|z(0)|=1$ and $\Phi(0)=\frac{\pi}{2}$ mod π, which is given by $(\kappa\cos\Phi)^2+z^2=1$, $\kappa=2C/3\beta\Psi_{\max}^2$, Eq. (35). Lines 1–8 correspond, respectively, to $k=0.5$, 0.8, 0.95, 1, 1.05, 1.25, 2, and 10. Lines 1–3 describe the self-trapped mode, line 4 describes the separatrix, and lines 5–8 describe the wandering breather or new tunneling mode of two weakly linked BECs.

$$(\kappa\cos\Phi)^2 + z^2 = 1, \tag{35}$$

where $\kappa=2C/3\beta\Psi_{\max}^2$; see Fig. 1.

With the use of Eq. (34), Eqs. (22) and (25)–(28) will take the following form:

$$\omega^2 = \omega_m^2 + \left(\frac{9}{2}\beta - 8\alpha^2\right)\Psi_{\max}^2 - k^2, \tag{36}$$

$$\dot{\Phi} = \frac{3}{2\omega}\beta\Psi_{\max}^2\cos(2\Theta), \quad \dot{\Theta} = \frac{C}{2\omega}\sin\Phi, \tag{37}$$

$$\dot{\Phi} = \frac{3}{2\omega}\beta\Psi_{\max}^2 z, \quad \dot{z} = -\frac{C}{\omega}\sqrt{1-z^2}\sin\Phi. \tag{38}$$

Finally, for two identical weakly coupled chains with $l^{(1)}=l^{(2)}=1$ and $\omega_m\approx 2$ we get from Eqs. (37) the following two equivalent physical-pendulum equations:

$$\ddot{\Xi} + \Omega_0^2\sin\Xi = 0 \tag{39}$$

for $\Xi=4\Theta$, where $\Omega_0=3\beta\Psi_{\max}^2/4$, and

$$\ddot{\delta} + \frac{C^2}{4}\sin\delta = 0 \tag{40}$$

for $\delta=2\Phi-\pi$. In the following we will solve Eq. (39) with the initial condition $\Theta(0)=0$, which corresponds to zero complex field Ψ_2 in the second chain at $t=0$ [or $z(0)=1$] and which is realized in our simulations. Therefore we will assume that $\Xi(0)=0$, $\Phi(0)=\frac{\pi}{2}$ mod π, and $\dot{\Xi}(0)=C$. The corresponding initial conditions for δ in Eq. (40) are $\delta(0)=0$ mod 2π and $\dot{\delta}(0)=\frac{3}{2}\beta\Psi_{\max}^2$.

The solution of the nonlinear physical-pendulum equation is well known (see, e.g., Ref. [48]) and can be written in terms of elliptic functions (with the elliptic modulus κ

$=2C/3\beta\Psi_{\max}^2$). Namely, one can obtain from Eq. (39) the following time evolution and fundamental oscillation frequency $\omega_{4\Theta}$ for $\Xi=4\Theta$:

$$4\Theta = 2\ \arcsin[\kappa\ \mathrm{sn}(\Omega_0 t,\kappa)], \quad \kappa \leq 1, \tag{41}$$

$$4\Theta = 2\ \arcsin[\mathrm{sn}(\kappa\Omega_0 t,1/\kappa)], \quad \kappa \geq 1, \tag{42}$$

$$\omega_{4\Theta} = \frac{\pi}{2}\frac{\Omega_0}{K(\kappa)}, \quad \kappa \leq 1, \tag{43}$$

$$\omega_{4\Theta} = \pi\frac{\Omega_0\kappa}{K(1/\kappa)}, \quad \kappa \geq 1, \tag{44}$$

where "sn" is the Jacobian elliptic sine and $K(\kappa)=F(\pi/2,\kappa)$ is a complete elliptic integral of the first kind. The solution for $\delta=2\Phi-\pi$ can also be found with the use of Eq. (40).

The important property of the solution of the physical-pendulum Eq. (39) [or (40)] is the existence of two qualitatively different dynamical regimes of Eqs. (37) and (38), which are detached by a separatrix corresponding to the condition $\kappa=1$ or $3\beta\Psi_{\max}^2=2C$.

For $\kappa \gg 1$ or $\beta\Psi_{\max}^2 \ll 2C/3$, the parameter Θ linearly grows with the "running" time $\tilde{t}\equiv t-\frac{k}{\omega}x$, while $\Phi\approx\Phi(0)=\frac{\pi}{2}$ (see, e.g., Ref. [49]):

$$\Theta \approx \tilde{C}\frac{\tilde{t}}{4} + \frac{9\beta^2\Psi_{\max}^4}{64\tilde{C}^2}\sin(\tilde{C}\tilde{t}),$$

$$\Phi \approx \frac{\pi}{2} + \frac{3\beta\Psi_{\max}^2}{2\tilde{C}}\sin\left(\tilde{C}\frac{\tilde{t}}{2}\right),$$

$$z \approx \cos\left(\tilde{C}\frac{\tilde{t}}{2}\right),$$

$$\tilde{C} = C - \frac{\Omega_0^2}{C} = C - \frac{9\beta^2\Psi_{\max}^4}{16C}. \tag{45}$$

In this regime Θ spans the full range from 0 to 2π, which, according to Eqs. (19) and (20), corresponds to the *complete* energy exchange between the nonlinear chains and therefore to the breather, wandering between the two chains. According to Eq. (21), the flux of the interchain energy exchange in this regime, $J_1 \propto C\Psi_{\max}\sin 2\Theta \sin\Delta = C\Psi_{\max}\sin(\tilde{C}\tilde{t}/2)$, has the rate $\omega_{beat}=\tilde{C}/2=[C-9\beta^2\Psi_{\max}^4/(16C)]/2$ for $\kappa \gg 1$, which continuously decreases with the increase of the ratio $\beta\Psi_{\max}^2/C$ below the separatrix. Since $\langle\cos\Theta^2\rangle=\langle\sin\Theta^2\rangle=1/2$ in this mode, the time-averaged inverse localization lengths $\lambda_{1,2}$, Eq. (23), are equal in the two chains: $\lambda_1=\lambda_2=\Psi_{\max}\sqrt{3\beta-8\alpha^2}$ (for $3\beta>8\alpha^2$; see Sec. III A below).

This dynamical regime is analogous to the complete energy exchange in the beating in a system of two coupled harmonic oscillators. The solution $\Theta=C\tilde{t}/4$, $\Phi=\frac{\pi}{2}$, and $z=\cos(C\tilde{t}/2)$ can be obtained directly from the linearized equations (14).

A similar tunneling mode can also be realized for BECs in a symmetric double-well potential when the condensate is initially loaded into one of the wells, $z(0)=\pm 1$; cf. Ref. [29]. In such a mode the relative phase of the coupled BECs will oscillate around $\frac{\pi}{2}$ mod π [see Eq. (45) and Fig. 1], which can be observed by means of interference. This tunneling mode is similar to but is different from the mode of Josephson plasma oscillations, already realized in experiments [31], in which the relative population imbalance is always less than 1 and the relative phase of the coupled BECs oscillates around 0 (mod 2π). The substantial difference between the time evolution of the average relative phase in the tunneling mode observed in [31] and in the mode predicted in Fig. 1 is caused by the difference in the initial states (population imbalance and relative phase) of two weakly linked Bose-Einstein condensates: it is $|z(0)|<1$ and $\Phi(0)=0$ mod 2π in the former case while it is $|z(0)|=1$ and $\Phi(0)=\pi/2$mod π in the latter case.

It is worth emphasizing that according to Eqs. (19), (20), and (45), the temporal Fourier spectrum of the wandering breather is determined both by the frequency ω and time dependence of Θ. The latter produces in the spectral density of the wandering breather a series of doublets of frequencies, shifted upward and downward with respect to the fundamental breather frequency ω: $\omega\pm n\omega_{beat}=\omega\pm n\tilde{C}/2$, $n=1,2,\ldots$; see Eq. (45). The lower frequencies in such doublets can become less than the threshold frequency ω_m in the phonon band of the coupled chains (see the dashed line in Fig. 8 below), which results in weak damping of the coupled nonlinear oscillations caused by the emission of small-amplitude phonons in the chains.

In the opposite limit $k \ll 1$ or $\beta\Psi_{\max}^2 \gg 2C/3$, one has

$$\Theta \approx \frac{C}{3\beta\tilde{\Psi}_{\max}^2}\sin\left(\frac{3}{4}\beta\tilde{\Psi}_{\max}^2\tilde{t}\right),$$

$$\Phi \approx \frac{\pi}{2} + \frac{3}{4}\beta\tilde{\Psi}_{\max}^2\tilde{t} + \frac{C^2}{18(\beta\Psi_{\max}^2)^2}\sin\left(\frac{3}{2}\beta\tilde{\Psi}_{\max}^2\tilde{t}\right),$$

$$z \approx 1 - \frac{2C^2}{9(\beta\tilde{\Psi}_{\max}^2)^2}\sin^2\left(\frac{3}{4}\beta\tilde{\Psi}_{\max}^2\tilde{t}\right),$$

$$\beta\tilde{\Psi}_{\max}^2 = \beta\Psi_{\max}^2 - \frac{C^2}{9\beta\Psi_{\max}^2}. \tag{46}$$

In this mode the interchain energy exchange between the coupled chains is incomplete since always $\Theta \ll 1$ [cf. Eqs. (19) and (20)]. With the increase of the ratio $\beta\Psi_{\max}^2/C$ beyond the separatrix, the flux of such incomplete energy exchange, $J_1 \propto (C^2/\Psi_{\max})\sin 2\Theta \sin\Phi = (C^2/2\Psi_{\max})\times\sin(3\beta\tilde{\Psi}_{\max}^2\tilde{t}/2)$ [cf. Eq. (21)], gradually decreases, but its rate $3\beta\tilde{\Psi}_{\max}^2/2$ gradually increases [see Eq. (46)]. This mode is similar to the macroscopic quantum self-trapping of interacting Bose-Einstein condensates in a single-bosonic Josephson junction [29,31–33], as well as to the asymmetric nonlinear mode (known, e.g., for two coupled nonlinear waveguides [43,50,51]), in which one system, here system 1,

carries almost all vibrational energy while the other one is almost at rest.

The separatrix $k=1$ or $\beta\Psi_{\max}^2=2C/3$ is characterized by zero frequency of the physical pendulum (39) [or (40)], which corresponds to the infinite period of the interchain energy exchange. For the initial conditions considered, the separatrix is described by the following solution of Eqs. (37) and (38):

$$\Theta = \arctan\left[\exp\left(\frac{C}{2}t\right)\right] - \frac{\pi}{4},$$

$$\Phi = 2\arctan\left[\exp\left(\frac{C}{2}t\right)\right],$$

$$z(0) = 1, \quad z(\infty) = 0,$$

$$\Phi(0) = \frac{\pi}{2}, \quad \Phi(\infty) = \pi. \tag{47}$$

The flux of the interchain excitation exchange is zero at the separatrix for $t\to\infty$: $J_i=0$ since $\sin\Phi=0$; see Eq. (21). On the other hand, the breather frequency ω is finite at the separatrix and is equal to

$$\omega_{sep} = \omega_m + (9\beta/8 - 2\alpha^2)\Psi_{\max}^2 - k^2/4$$
$$\approx 2 + C - 2\alpha^2\Psi_{\max}^2 - k^2/4, \tag{48}$$

since $3\beta\Psi_{\max}^2=2C$ at the separatrix and $\omega_m\approx 2+C/4$; see Eqs. (12), (19), (20), and (36). The value $\omega_{sep}=\sqrt{4+4C}\approx 2.0976$ for $C=0.1$, $\alpha=0$, and $k\ll 1$ coincides with very good accuracy with the one, $\omega_{sep}\approx 2.098$, which follows from our numerical simulations of the separatrixlike dynamics of the wandering breather in two coupled β-FPU chains; see Figs. 7 and 11 below. In corresponding dimensionless units, the above separatrix, Eq. (47), gives the position, in terms of the spatial soliton amplitude and interfiber coupling, of the numerically revealed separatrixlike regime between the regimes of the total and partial exchange of photon energy between two coupled nonlinear optical fibers (fiber directional coupler), described by two coupled nonlinear Schrödinger equations [52]. The existence of a separatrix was revealed in different models of nonlinear dimer (two coupled nonlinear systems with two degrees of freedom), both classical and quantum, in Refs. [42–44,53,54].

The important result of our studies in this field is that the dynamics of two coupled nonlinear systems with many degrees of freedom (two weakly coupled low-amplitude and macroscopically wide breathers) can be (approximately) mapped onto the dynamics of the exactly solvable nonlinear dimer. The (macroscopically) large number of degrees of freedom in the considered coupled systems allows also one to consider their relative phase Φ as an observable quantity, as in the case of weakly coupled interacting Bose-Einstein condensates [31].

It is worth mentioning that the form and corresponding frequency of a breather in an *isolated anharmonic chain* can be obtained in our model only in the self-trapping breather regime, in which one can consider the limit of $C\to 0$. Indeed, as follows from Eq. (46), in this limit one has $\Theta=0$ ($z=1$) and the breather frequency, according to Eqs. (19), (20), and (36), is equal to

$$\omega(\Psi_{\max},k) = \omega_m + \left(\frac{9}{8}\beta - 2\alpha^2\right)\Psi_{\max}^2 + \frac{3}{8}\beta\Psi_{\max}^2 - \frac{1}{4}k^2$$
$$= 2 + \left(\frac{3}{2}\beta - 2\alpha\right)\Psi_{\max}^2 - \frac{1}{4}k^2. \tag{49}$$

This expression for the breather frequency is fully consistent with the known expression for the frequency of an immovable or slowly moving breather in a single α-β-FPU chain in the small-amplitude limit; see, e.g., Refs. [2,21]. It is important to emphasize that to get this expression for breather frequency ω, we have explicitly taken into account the linear increase in time (*winding up*) of the relative phase $-\Phi/2$ in Eq. (19), given by Eq. (46) in the self-trapping regime. A similar winding up of the relative phase of two coupled interacting Bose-Einstein condensates in the nonlinear self-trapping mode has been recently measured directly in a single-bosonic Josephson junction by means of interference [31]. This finding gives us an additional argument in favor of the similarity between the macroscopic tunneling quantum dynamics and phase-coherent dynamics of weakly coupled breathers.

III. NUMERICAL SIMULATIONS AND COMPARISON WITH ANALYTICAL PREDICTIONS

To simulate the dynamics of coupled nonlinear lattice excitations, we numerically integrate Eqs. (2) for two identical chains, $l^{(1)}=l^{(2)}=1$, $\alpha^{(1)}=\alpha^{(2)}\equiv\alpha$, and $\beta^{(1)}=\beta^{(2)}\equiv\beta$, with absorbing edge conditions. We use the latter conditions in order to get rid of weak radiation, caused by the wandering breather (because such radiation will stay in the system forever in the case of periodic boundary conditions). For the convenience of the numerical simulations, the Fermi-Pasta-Ulam Hamiltonian (1) for two coupled chains with N particles can be written in the following equivalent dimensionless form:

$$H = \sum_{i=1}^{2}\left[\sum_{n=1}^{N}\frac{1}{2}u_n^{(i)2} + \sum_{n=1}^{N-1}V(u_{n+1}^{(i)} - u_n^{(i)}) + \sum_{n=1}^{N}U(u_n^{(i)} - u_n^{(3-i)})\right], \tag{50}$$

where the potentials $V(x)$ and $U(x)$ describe, respectively, the intra- and interchain interactions. We normalize the dimensionless potential $V(x)$ with the conditions $V(0)=V'(0)=0$ and $V''(0)=1$, while the potential $U(x)$ we normalize with the conditions $U(0)=U'(0)=0$ and $U''(0)=C>0$. According to Eq. (1), we take the following form for the intra- and interchain potentials:

$$V(x) = \frac{1}{2}x^2 + \frac{1}{3}\alpha x^3 + \frac{1}{4}\beta x^4, \tag{51}$$

$$U(x) = \frac{1}{2}Cx^2, \tag{52}$$

with $C=0.1$ describing the strength of the weak interchain coupling.

Then the equations of motion (2) will take the form as

$$\ddot{u}_n^{(i)} = F(r_n^{(i)}) - F(r_{n-1}^{(i)}) + G(\delta_n^{(i)}), \tag{53}$$

where $r_n^{(i)} = u_{n+1}^{(i)} - u_n^{(i)}$, $\delta_n^{(i)} = u_n^{(3-i)} - u_n^{(i)}$, $i=1,2$, $F(r) = V'(r) = r + \alpha r^2 + \beta r^3$, and $G(\delta) = U'(\delta) = C\delta$.

We search for the localized nonlinear lattice excitation (discrete breather) as a solution of a set of the nonlinear equations $\mathcal{F}(\mathbf{X})=\mathbf{0}$, where the vector $\mathbf{X}=\{u_n^{(i)}(0), \dot{u}_n^{(i)}(0)\}_{i=1,n=1}^{2,N}$ gives the initial values for the localized nonlinear lattice excitation (discrete breather) as a solution of a set of nonlinear equations (53), while the vector $\mathcal{F}(\mathbf{X}) = \{u_n^{(i)}(t_p) - u_n^{(i)}(0),\ \dot{u}_n^{(i)}(t_p) - \dot{u}_n^{(i)}(0)\}_{i=1,n=1}^{2,N}$ gives the change of the vector $\mathbf{X}$ during the one period of breather oscillations $t_p = 2\pi/\omega$. To find the value of $\mathcal{F}(\mathbf{X})$, one needs to integrate Eqs. (53) numerically during the time interval $[0, t_p]$. The use of such numerical method for finding of an exact breather solution is explained in details in Ref. [10]. The main difficulty in this numerical method is to find an appropriate initial vector $\mathbf{X}$ for the subsequent iterative solution of the nonlinear equations (53).

The vibrational energy of the breather is determined correspondingly as

$$E = \sum_{i=1}^{2}\left[\frac{1}{2t_p}\sum_{n=1}^{N}\int_0^{t_p}\left(\dot{u}_n^{(i)2} + V(r_n^{(i)}) + V(r_{n-1}^{(i)}) + \frac{1}{2}C\delta_n^{(i)2}\right)dt\right] \equiv \sum_{i=1}^{2} E_i. \tag{54}$$

A. Simulation of dynamics of discrete breathers in two weakly coupled chains

Equations (53) for two coupled chains can be reduced to the equations for one chain in the case of symmetric, $u_{n,1} \equiv u_{n,2} \equiv u_n$, and antisymmetric, $u_{n,1} = -u_{n,2} \equiv u_n$, motion in the chains. In the symmetric case the Hamiltonian (50) has the usual form for a single FPU chain:

$$H = 2\sum_{n=1}^{N}\left\{\frac{1}{2}\dot{u}_n^2 + V(u_{n+1} - u_n)\right\}. \tag{55}$$

For the symmetric intrachain potential $V(r)$—i.e., for $\alpha=0$—equations of motion in a system of two chains can also be reduced to the one-chain equations in the case of antisymmetric (antiphase) motion in the chains. In this case the reduced system has a standard Hamiltonian of the FPU chain on an external harmonic substrate:

$$H = 2\sum_{n=1}^{N}\left\{\frac{1}{2}\dot{u}_n^2 + V(u_{n+1} - u_n) + 2Cu_n^2\right\}. \tag{56}$$

Discrete breathers in such a chain with $C \geq 0$ were studied in detail; see, e.g., Ref. [10]. In the system with Hamiltonian (56), either with $C=0$ or $C>0$, there are two types of discrete breathers with frequency $\omega > \omega_{\max} \equiv \sqrt{4+2C}$; see, e.g., Refs. [3–5]. The center of symmetry of the breather coincides with a given lattice site in one breather type, and it coincides with a middle point between two neighboring sites in another type. In both cases of the symmetric and antisymmetric breathers in the coupled chains, the vibrational energy of the nonlinear excitation, Eq. (54), is equally distributed between the chains. Numerical analysis of Eqs. (53) reveals that besides these nonlinear eigenmodes there is an "asymmetric" mode in which only one chain is involved in the vibrations while the vibrations of the other chain "adiabatically" follow the vibrations of the main one. The characteristic form of the displacement patterns in one- and two-chain antisymmetric breathers is shown in Fig. 2, while the dependence of their energies on breather frequency ω is shown in Fig. 3.

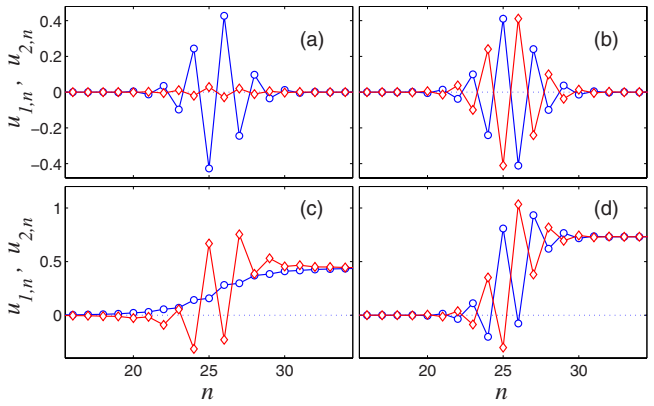

FIG. 2. (Color online) Displacement patterns for (a) one-chain breather and (b) two-chain antisymmetric breather with frequency $\omega=2.3$ for the quartic intrachain anharmonic potential ($\alpha=0$, $\beta=1$); (c) and (d) show displacement patterns for one-chain and two-chain breathers, respectively, in the presence of cubic and quartic intrachain anharmonic potentials ($\alpha=-1$, $\beta=1$) for the same breather frequency. The patterns for the first and second chains are indicated by open circles and open diamonds, respectively, and are shown at the moments when all particle velocities are zero.

As we can see from a comparison of Figs. 2(c) and 2(d), the magnitudes of the static displacement kinks in the center-of-mass displacement differences $\Delta w_0^{(\mathrm{c.m.})} = w_0^{(\mathrm{c.m.})}(+\infty) - w_0^{(\mathrm{c.m.})}(-\infty)$ differ almost twice for the two- and one-chain breathers in coupled chains with cubic intrachain anharmonic potential. This is in accordance with the prediction of Eqs. (9) and (10) that the ratio of such magnitudes is given mainly by the ratio of the total vibrational energies of the corresponding breathers. As follows from Fig. 3(c), the ratio of the (total vibrational) energies of the two- and one-chain breathers for $\omega=2.3$, $\alpha=-1$, and $\beta=1$ is indeed close to 2.

In the absence of the cubic anharmonic intrachain potential ($\alpha=0$, $\beta=1$), the energy of the antisymmetric two-chain breather monotonously increases from zero, for $\omega=\omega_{\max} = \sqrt{4+2C} \approx 2.05$, to the infinity for $\omega \to \infty$; see Fig. 3(a). There is only one type of antisymmetric two-chain breather for low frequencies $\omega_{\max} < \omega < 2.066$, but at $\omega = 2.066 \equiv \omega_{bif}$ the antisymmetric two-chain breather bifurcates and the one-chain breather mode detaches from the two-chain

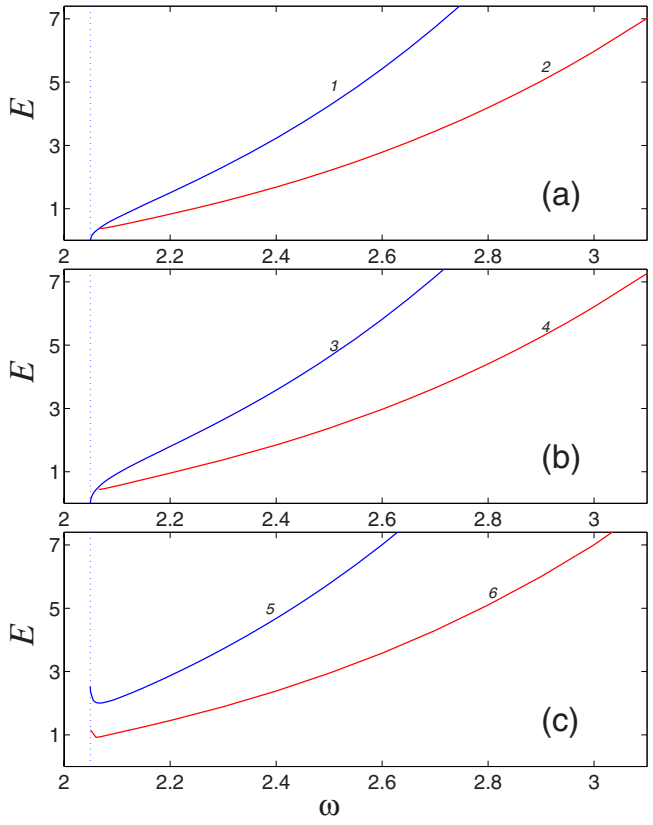

FIG. 3. (Color online) Dependence of breather energy E in a system of two coupled chains on breather frequency ω for different strengths of cubic intrachain anharmonic potential: $\alpha=0$ (a), $\alpha=-0.5$ (b), and $\alpha=-1$ (c), with the same strength of quartic anharmonic potential $\beta=1$. Lines 1, 3, and 5, correspond to antisymmetric two-chain breathers; lines 2, 4, and 6 correspond to one-chain breathers. All the lines correspond to the breathers with centers of symmetry located in the middle of two nearest particles; cf. Figs. 2(a)–2(d). The dotted vertical line in all the plots shows the upper boundary of phonon spectrum in the two-chain system, $\sqrt{4+2C} \approx 2.05$.

mode. The one-chain breather exists for all frequencies $\omega > \omega_{bif}$.

We can get an analytical estimate for the characteristic frequency ω_{bif} with the use of the generic evolution equations (27) and (28). Indeed, for positive β, $\Phi=\pi$, and $\omega_{m1}=\omega_{m2}$ one has an equation for the steady state, with $\dot{\Theta}=0$ and $\dot{\Phi}=0$, the dynamical state in the coupled chains:

$$\sqrt{1-z^2} = \frac{C}{3\beta\Psi_{\max}^2}, \tag{57}$$

which has a solution for real z only for $3\beta\Psi_{\max}^2 \geq C$. Using this condition and Eq. (36) for the breather frequency, in the case of $\alpha=0$ and $k=0$, we get the following expression for ω_{bif} at the appearance of the new solution (for $C=0.1$):

$$\omega_{bif} = \sqrt{4+\frac{5}{2}C} = \sqrt{4.25} = 2.062, \tag{58}$$

which coincides with good accuracy with the numerically revealed value $\omega_{bif}=2.066$. As follows from Eq. (57), at the bifurcation point $3\beta\Psi_{\max}^2=C$ one has $z=0$. This corresponds to the equal populations of the coupled chains, which in turn results in equal energies of the two- and one-chain breather solutions at the bifurcation point; see Fig. 3(a).

Two types of the coupled breathers, the one- and two-chain breathers, can exist also in the presence of a cubic term in the anharmonic intrachain potential $V(x)$, Eq. (51). The effect of the cubic term in the anharmonic intrachain potential on the breather dynamics in a single FPU chain was studied in Refs. [2,39–41,55]. For instance, it was shown in Ref. [2] that low-amplitude breathers can exist in a single FPU chain only in the case of relatively weak cubic anharmonic term in the intrachain potential $V(x)$—namely, when $\alpha < \sqrt{3\beta/4}$. (For the case considered of $\beta=1$, this requirement reduces to $\alpha < \sqrt{3/4}=0.866$.) In fact, this requirement corresponds to the requirements $\omega > \omega_m$ in Eq. (49) and $\lambda_1^2 > 0$ in Eq. (23) for the breather frequency and inverse localization length in a single FPU chain (for $\Theta=0$ and $k=0$).

From our analysis we can conclude that bifurcation of breather modes in two weakly coupled nonlinear chains with cubic intrachain anharmonic potential occurs only for $\alpha < \sqrt{3\beta/8}$. For larger cubic intrachain anharmonic potential $\alpha > \sqrt{3\beta/8}$, there are no low-amplitude breathers in the coupled chains, but there are finite-amplitude breathers with a threshold in energy which does not go to zero for $\omega \to \omega_{\max}+0$; see Fig. 3(c) and cf. Fig. 4 in Ref. [55]. Indeed, from Eq. (23) it follows that for the wandering breather, when $\langle \cos^2\Theta \rangle = \langle \sin^2\Theta \rangle = 0.5$, the inverse localization lengths $\lambda_{1,2}$ are real positive only for $\alpha < \sqrt{3\beta/8}$, when the above picture of the breather periodic translation (wandering) between the coupled chains takes place. On the other hand, for $\alpha > \sqrt{3\beta/8}$ (or $\alpha > 0.61$ in the case considered), one has to take into account the contribution to the breather frequency ω and inverse square localization lengths $\lambda_{1,2}^2$ of the finite-amplitude breather of the terms $\propto \Psi_{\max}^4$ (with positive coefficients). These terms will result in a finite (threshold) energy of the breather with minimal possible frequency $\omega_{\min} > \omega_m$. According to Eqs. (14), the existence of such a threshold breather amplitude and energy in the coupled chains with $\alpha > \sqrt{3\beta/8}$ is related with the static strain in both chains ($\partial w_0^{(\mathrm{c.m.})}/\partial x = -\alpha\langle |\Psi_1|^2 + |\Psi_2|^2 \rangle$), which accompanies breathers in coupled chains with nonsymmetric anharmonic potentials and which is localized around the central region of the breather; see Eqs. (9) and (10) and Figs. 2(c) and 2(d).

In the coupled chains with $\alpha > \sqrt{3\beta/8}$, there is no bifurcation of the two-chain breather mode: there are two separated breather modes, the one- and the two-chains ones, for all the frequencies $\omega > \omega_{\min}$. The energy of the two-chain breather mode is always larger than the energy of the one-chain one, and there are thresholds in energies for both types of the breathers; see Fig. 3(c). In the following we will restrict ourselves only to the case of weakly coupled β-FPU chains with zero cubic anharmonic intrachain potential and assume everywhere below that $\alpha=0$ and $\beta=1$.

For the large-amplitude (high-frequency) nonlinear oscillations in two weakly coupled β-FPU chains, there are many coupled (bound) antisymmetric breather modes whose strongly localized displacement patterns are shifted one with respect to another along the chains; see Figs. 4(a)–4(j). In

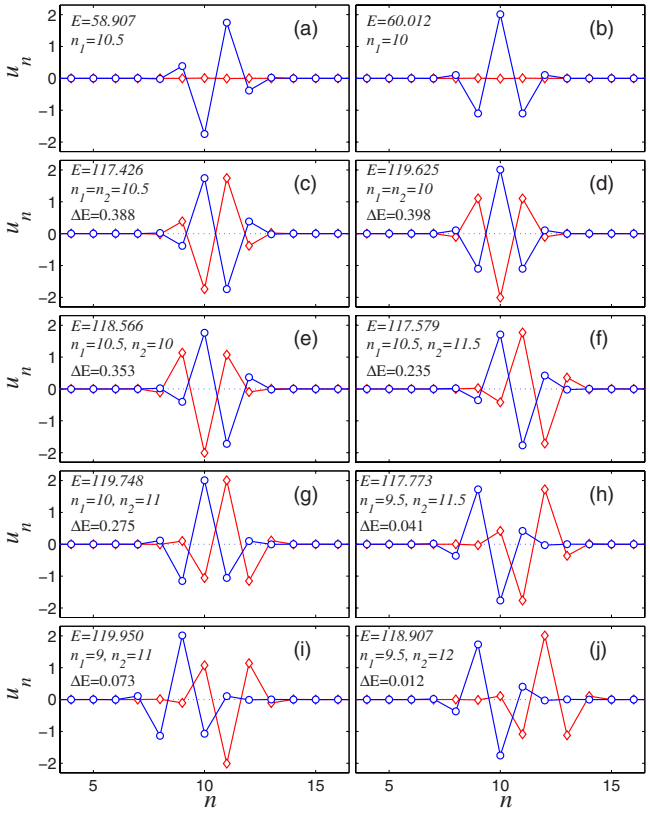

FIG. 4. (Color online) Displacement patterns for two-chain breathers with $\omega=5$ in a system of two chains with pure quartic intrachain anharmonic potential, with $\alpha=0$, $\beta=1$. The patterns for the first and second chains are indicated by open circles and open diamonds, respectively, and are shown at the moments when all particle velocities are zero. Here E is the breather energy, n_1 and n_1 are the locations of the center of symmetry of the breather in the ith chain, and $\Delta E=E_1^{(1ch)}+E_2^{(1ch)}-E$ is the gain in energy due to breather coupling (breather "binding energy").

these figures the total breather energy E, Eq. (54), the location of the breather center in the corresponding chain, and the "binding energy"—i.e., the gain in energy due to breather coupling, $\Delta E=E_1^{(1ch)}+E_2^{(1ch)}-E$—are indicated for breathers with (high) frequency $\omega=5$. Here $E_{1,2}^{(1ch)}$ indicate the energy of the corresponding one-chain breather located in the corresponding chain; see Figs. 4(a) and 4(b) for the two main types of the one-chain breathers: with the center of symmetry placed in the middle of two neighboring sites or in a particular site. As is seen from Fig. 4, the binding energy depends on the type of the bound breathers and apparently decreases with an increase of the interbreather distance (along the chains). Besides such one-frequency coupled breather modes, there are also two-frequency nonlinear modes which bind together large-amplitude breather modes in two chains with different but *commensurate frequencies* ω_1 and $\omega_2>\omega_1$. The dependence of the energy of several types of such commensurate-frequency bound breather modes on their maximal frequency ω_2 is shown in Fig. 5.

We also study the interaction of breathers in two weakly coupled β-FPU chains. For this purpose, we numerically integrate equations of motion (53) with the initial conditions which describe a breather with frequency ω_1 in the first chain

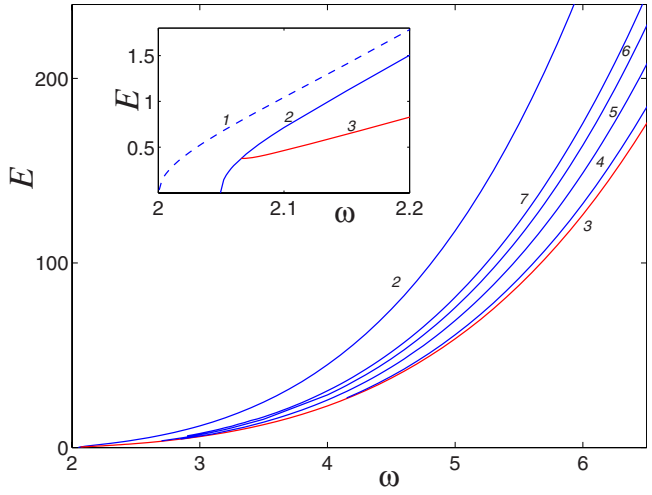

FIG. 5. (Color online) Breather energy E in a system of two chains versus frequency ω. Dashed line 1 in the inset corresponds to symmetric two-chain breather, line 2 describes two-chain antisymmetric breather, and line 3 describes a one-chain breather. Lines 4–7 in the main plot correspond to two-chain excitations which couple breathers with two different commensurate frequencies with ratios $\omega_1:\omega_2=1:2$, $\omega_1:\omega_2=2:3$, $\omega_1:\omega_2=3:4$, and $\omega_1:\omega_2=4:5$, respectively. Frequency ω in the plot always denotes maximal frequency ω_2.

and a breather with frequency ω_2 in the second chain. In Fig. 6 we show the change in time of the spectral density $p(\omega)$ of the emerged localized vibrational mode in the coupled neighboring chains with two breathers with initial frequencies $\omega_1=2.6$ and $\omega_2=3$. As one can see in this figure, a two-frequency breather is generated in the system with the ratio of frequencies $\omega_1:\omega_2=6:7$, which subsisted for 1200 units of dimensionless time (when time is measured in units in which $\omega_m=\sqrt{4+C}\approx 2$). Later the breather with higher frequency (and energy) starts to adsorb the energy of the breather with smaller frequency (and energy), which decreases the frequency of the latter. As a result, the one-chain breather with frequency $\omega=3.160$ is formed. Hence the breather with higher energy completely adsorbs the breather with smaller energy. This recalls the *merging* of low-

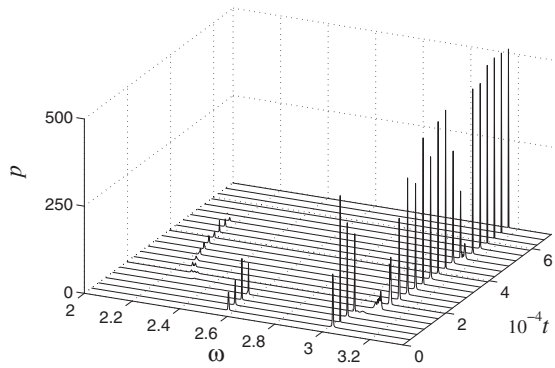

FIG. 6. Time evolution of the spectral density $p(\omega)$ of the nonlinear localized excitation of two weakly coupled chains under the initial excitation of a breather with frequency $\omega_1=2.6$ in one chain and a breather with frequency $\omega_2=3$ in another chain.

amplitude (small-energy) breathers in a single 1D β-FPU chain, which results in a single localized object (discrete breather) containing almost all of the initial total vibrational energy of the lattice [21]. If we initially prepare two breathers with more close initial frequencies $\omega_1=2.7$ and $\omega_2=3$, a two-chain one-frequency breather with antisymmetric displacement pattern is formed (not shown). In this case the interaction and energy exchange of the two breathers with initially different frequencies result in frequency equalization. Therefore our simulations show that despite the existence of the coupled two-frequency breathers, the one-frequency coupled breather modes are in general more stable.

B. Simulation of wandering breathers in two weakly coupled chains

Here we will study the dynamics of two weakly coupled chains under excitation of a breather only in one chain while keeping the other chain initially at rest. This amounts to numerical integration of Eqs. (53) for chain 1 under the initial conditions $u_n^{(2)}=0$ and $\dot{u}_n^{(2)}=0$. As a result of the interchain interaction, the excitation initially located in one chain can start to periodically translate (wander) between the coupled chains. Such an interchain energy exchange can be studied quantitatively by measuring the time dependence of the energy E_i in each chain; see Eq. (54).

In Fig. 7 we plot the energy of each chain E_i as a function of time when the immovable breather (with $V=0$) is excited in chain 1 with a given frequency ω. For relatively small breather amplitude and corresponding dimensionless breather frequency, $\omega=2.030>\omega_m=\sqrt{4+C}=2.025$, an almost complete interchain energy exchange occurs when the total breather energy $E=E_1+E_2$, Eq. (54), is periodically located in one of the coupled chains; see Fig. 7(a). From this figure we can measure the period of wandering T_w, which is close to 126. Taking into account that the frequency of the complete interchain energy exchange for the small-amplitude breather is equal to $C/2=0.05$ [see Eqs. (21) and (45)], the wandering period T_w is equal to $4\pi/C=125.66$, which coincides to very high accuracy with the period, which can be found from Fig. 7(a). With the increase of breather amplitude and frequency, the period of the interchain energy exchange increases, in accordance with Eq. (45), but the exchange remains complete up to the critical breather frequency (and corresponding amplitude), which according to Figs. 7(b) and 7(c) is very close to $\omega=2.0980$. This critical breather frequency should be compared with the value of frequency of the immovable breather at the separatrix, $\omega_{sep}=\sqrt{4+4C}=2.0976$ for $C=0.1$, $\alpha=0$, and $k=0$ [see Eq. (48)], which also shows very good agreement with the prediction of the approximate physical pendulum, Eq. (39) [or (40)]. For the higher breather frequencies $\omega>2.098$ (and corresponding breather amplitudes), the interchain energy exchange is no longer complete and corresponds to the exchange of relatively small fraction of the total breather energy E; see Figs. 7(c) and 7(d). For $\omega=2.1106$, the main part of the breather energy remains all the time in chain 1 where the breather was initially excited, which corresponds to nonlinear self-trapping of the breather; see Fig. 7(d). The transition from the oscillatory energy exchange, Fig. 7(b), to the self-trapped mode, Fig. 7(c), is very sharp: the change of breather frequency by the crossing of the separatrix occurs to the fifth digit only. One can also see a large difference in energy exchange rate in the wandering breather mode, Fig. 7(a), and in the separatrix mode, Figs. 7(b) and 7(c): with the change of the breather frequency from $\omega=2.0300$ to $\omega=2.098$, the rate of energy exchange decreases more than 20 times. This observed feature of the coupled nonlinear systems is also in perfect accordance with the prediction of the physical pendulum, Eq. (39) [or (40)] for the separatrix mode with the infinite period of the interchain energy exchange, described by Eq. (47).

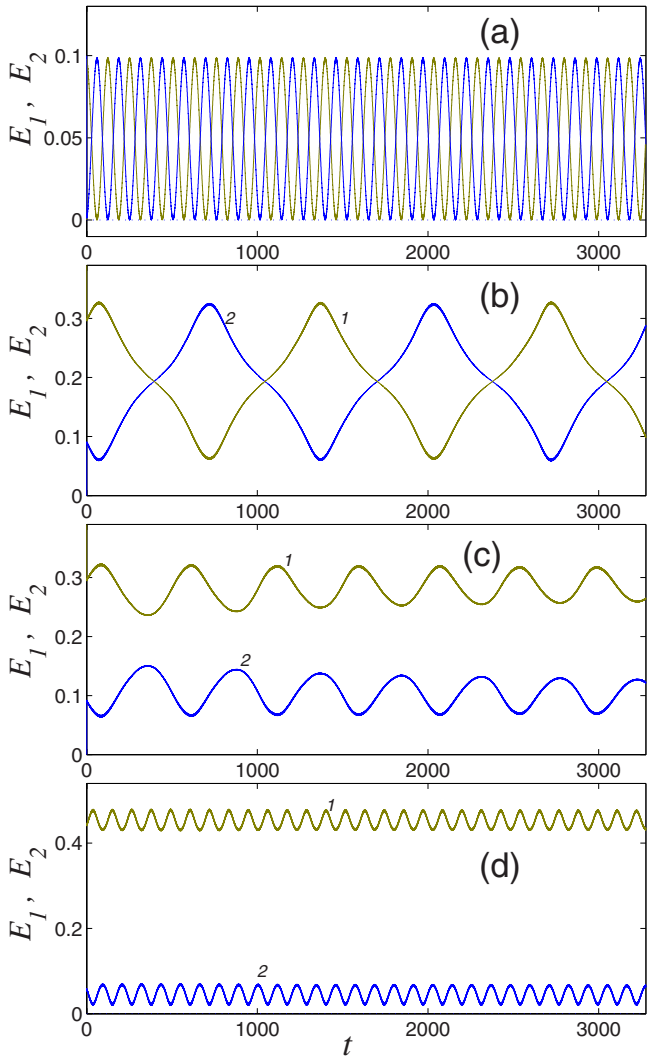

FIG. 7. (Color online) Time evolution of chain energies E_1 (green, light gray) and E_2 (blue, dark gray) of immovable breather in chains 1 and 2 versus time t, obtained from numerical solution of Eqs. (53) with the initial breather excitation in chain 1 (for immovable chain 2) with frequency (a) $\omega=2.0300$, (b) $\omega=2.0980$, (c) $\omega=2.0981$, and (d) $\omega=2.1106$. Two identical chains with $\alpha=0$, $\beta=1$, and $C=0.1$ and absorbing edges were used in simulations. The separatrix solution of Eq. (39) corresponds to $\omega=2.0976$. Time evolution is shown after $t=10^5$ from the excitation instant when all transients died out.

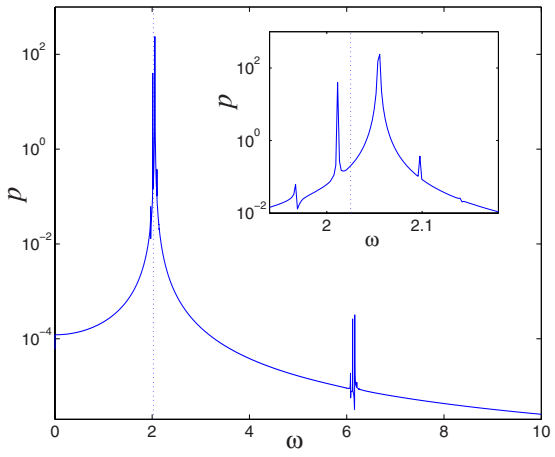

FIG. 8. (Color online) Spectral density $p(\omega)$ of a wandering breather in a system of two weakly coupled chains under the initial excitation of a breather with frequency $\omega=2.05$. The dotted vertical line indicates the upper bound of phonon frequency $\omega_m=\sqrt{4+C}\approx 2.025$ in Eqs. (14). The inset shows fine details of the spectral density in close vicinity of the fundamental breather frequency.

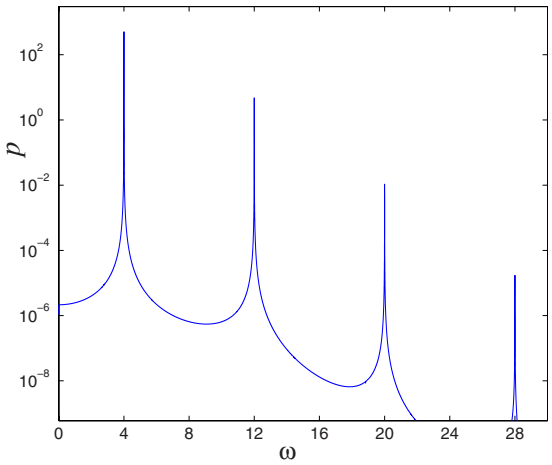

FIG. 9. (Color online) Spectral density $p(\omega)$ of a one-chain large-amplitude breather with frequency $\omega=4$ (in the self-trapped regime) in two coupled chains with $C=0.1$, $\alpha=0$, and $\beta=1$.

In Fig. 8 we show the Fourier power spectrum of the wandering breather. As was explained above in connection with the complex wave field of the wandering breather, Eqs. (19) and (20), the temporal Fourier spectrum of the wandering breather consists of the main peak at the breather fundamental frequency ω and its (upper and lower) frequency satellites at $\omega\pm n\omega_{beat}$, $n=1,2,\ldots$, where $\omega_{beat}\approx[C-9\beta^2\Psi_{\max}^4/(16C)]/2$ is the rate of complete interchain energy exchange in the wandering breather mode; see Eq. (45). The value of $\omega_{beat}\approx 0.05$ for low-amplitude wandering breathers in the chains with the coupling constant $C=0.1$ is in good agreement with the inset in Fig. 8. Therefore we can quantitatively reproduce both the numerically observed wandering (beating) period, Fig. 7(a), and wandering frequency, Fig. 8, of the low-amplitude and macroscopically wide breather.

The nonlinearity of the physical pendulum Eq. (39) [or (40)] results in all higher harmonics (second, third, etc.) of the beating frequency ω_{beat} and, respectively, in the appearance of the corresponding doublets of the breather frequency satellites: the satellites of the first and second harmonics of the beating frequency are clearly seen in the inset in Fig. 8. As we can also see in the inset in Fig. 8, the lower-side satellites enter the continuum of low-amplitude phonons, $\omega-n\omega_{beat}<\omega_m=\sqrt{4+C}=2.025$, $n=1,2,\ldots$. The latter means that the wandering breather (weakly) emits low-amplitude lattice phonons, which results in a (adiabatically slow) lowering of breather energy. This in turn means that the wandering breather is not an exact nonlinear eigenmode of two weakly coupled anharmonic chains, in contrast to the two-chain symmetric and antisymmetric breathers.

In Fig. 8 one can also see the third harmonic of the main breather frequency ω, which can be modeled with the use of the full harmonics, Eqs. (12) and (53), instead of Eqs. (14) written in the resonance approximation. For the β-FPU chain (with zero cubic anharmonic intrachain potential), there are only odd harmonics of the fundamental breather frequency. In a single chain, the higher harmonics of the fundamental breather frequency were first analytically predicted and described in Ref. [2] and were numerically observed, up to the ninth harmonic, in Ref. [22]. In Fig. 9 we show the power spectrum of the one-chain breather with frequency $\omega=4$ in the coupled chains with $\alpha=0$, $\beta=1$, and $C=0.1$. This spectrum clearly shows the existence of higher odd harmonics, up to the seventh one, of the fundamental frequency. Since the breather with such frequency is in the self-trapped mode in the considered coupled system ($\omega=4>\omega_{sep}\approx 2.1$), its dynamics and power spectrum are similar to the ones of the breather in a single chain; cf. Refs. [21,22]. Importantly, the Fourier spectrum in Fig. 9 corresponds to the almost "exact" breather solution found in the β-FPU chain with zero vibrational background, while the breather, studied in Refs. [21,22], was *self-assembled* on a nonzero vibrational background as a result of the modulational instability of the short-wavelength modes in the β-FPU chain.

In view of the present work, we can relate the doublets of satellites of the fundamental breather frequency (and its odd harmonics) in a *single chain* observed in Ref. [22] with the beating between two breather states with different center locations (and symmetry); see Figs. 4(a) and 4(b). According to these figures, the breather with the intersite center location, Fig. 4(a), has higher frequency than the breather with the same energy with the on-site center location, Fig. 4(b). According to the generic equation (27), the frequency difference under the proper initial conditions can cause breather wandering (beating) between two nearest lattice sites. The beating in turn can induce the steady-state translation of the breather along the chain with (slow) velocity $V\ll 1$, proportional to the (small) beating frequency (as was qualitatively explained in Ref. [22]). In Sec. III C we will discuss similar lateral translations of the 1D breather in a system of parallel weakly coupled nonlinear chains with transverse group velocity, proportional to the beating frequency in the case of two coupled chains. In contrast to the low-amplitude 1D breather, laterally moving and losing its energy due to phonon emission in a system of nonlinear chains [see Figs. 14(a) and 14(c) below], the high-frequency slowly moving

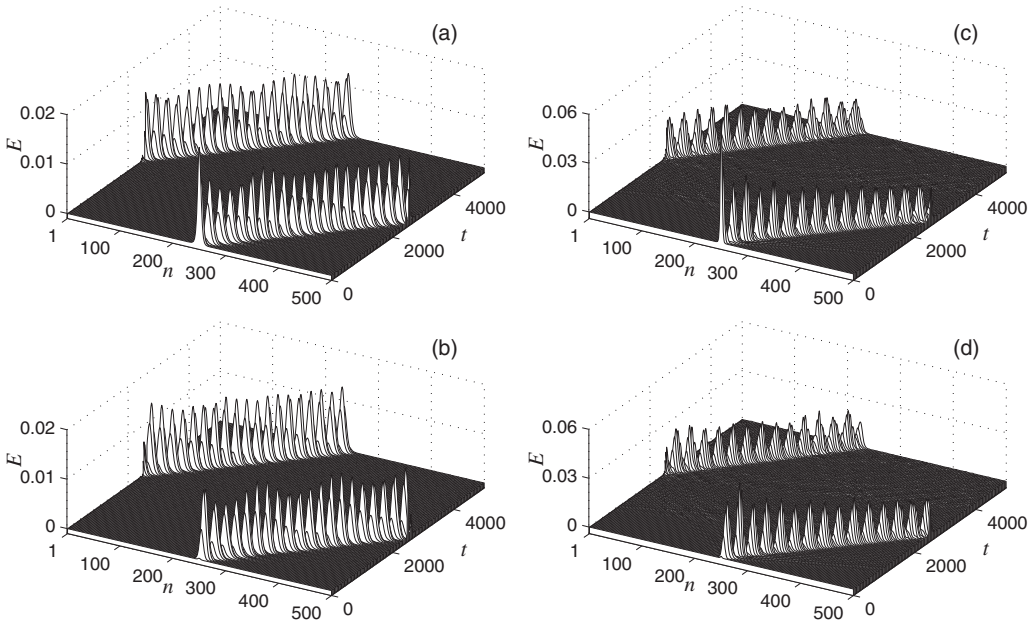

FIG. 10. Periodic translation of a slowly moving breather between two coupled chains with $C=0.1$, $\alpha=0$, and $\beta=1$. Time dependence of breather energy distribution in chain 1 [(a) and (c)] and chain 2 [(b) and (d)] is shown. The breather was initially excited in chain 1 with immovable chain 2, with velocity $V=0.1$ and amplitude $\Psi_{\max}=0.1$ [(a) and (b)] and with velocity $V=0.1$ and amplitude $\Psi_{\max}=0.2$ [(c) and (d)].

breather in a single chain does not emit phonons in the chain because the fundamental frequency satellites (caused by the beating) are all out of the phonon band; see Fig. 3 in Ref. [22].

A similar picture of the complete interchain energy exchange below the separatrix takes place also for the wandering breather, *slowly moving* along the chains. To model this effect, we numerically integrate Eqs. (53) with the initial conditions which correspond to the excitation of the moving in chain-1 breather solution, while keeping chain 2 at rest, with the following ansatz for lattice displacements:

$$u_n^{(1)}(t) = (-1)^n \Psi_{\max} \cos(kn - \omega t)/\cosh[\lambda(n - Vt)],$$

$$u_n^{(2)}(0) = 0, \quad \dot{u}_n^{(2)}(0) = 0, \tag{59}$$

where $\Psi_{\max}$, $\omega=\omega(\Psi_{\max},k)$, and $V\approx -k/\omega \ll 1$ are the amplitude, frequency, and slow velocity of the breather; cf. Eq. (19).

In Figs. 10 and 11 we show the energy, versus time and site, of a slowly moving breather, with velocity $V=0.1$, wandering between two weakly coupled chains. In Fig. 10 we show the energy of the wandering small-amplitude breather below the separatrix: with $\Psi_{\max}=0.1$, Figs. 10(a) and 10(b), and $\Psi_{\max}=0.2$, Figs. 10(c) and 10(d). Both figures show the complete interchain energy exchange. From Figs. 10(a) and 10(b) one can find that the period of complete interchain energy exchange (wandering) $T_w\approx 128$ for $\Psi_{\max}=0.1$ is very close to the one $T_w\approx 126$ in Fig. 7: both figures describe the almost harmonic wandering of a small-amplitude breather, with wandering frequency $C/2=0.05$. Below the separatrix, the wandering period T_w increases with breather amplitude: one has $T_w\approx 179$ for $\Psi_{\max}=0.2$ in Figs. 10(c) and 10(d). Figure 11 shows the dynamics of a slowly moving breather initially excited in chain 1 with amplitude $\Psi_{\max}=0.26$, which is very close to the one at the separatrix: $\Psi_{\max}^{(sep)}=\sqrt{2C/\beta}=0.2582$. Separatrixlike dynamics, similar to the one shown in Fig. 7(b), is well established for the later delay time $t\geq 4000$, when almost total energy of the moving breather periodically translates (wanders) between the chains. In Fig. 12 we show the dynamics of slowly moving breather, initially excited in chain 1 with velocity $V=0.1$ and amplitude $\Psi_{\max}=0.3$, which is beyond the separatrix. Here the interchain energy exchange is no longer complete, as in the case of an immovable breather beyond the separatrix [cf. Fig. 7(d)], but the period of such an exchange, $T_x\approx 125$, is much shorter than that close to the separatrix (cf. Fig. 11).

A slowly moving *wandering Bose-Einstein condensate* can be realized in two coupled 1D atom waveguides (see, e.g., Refs. [28,56]), for the BEC of weakly interacting atoms with non-negligible interwaveguide tunneling coupling and with total initial population imbalance $|z(0)|=1$.

Therefore the initial excitation of the low-amplitude (low-frequency) breather, either immovable or slowly moving, in one chain always results in its periodic transverse translation (wandering) between the two weakly coupled chains. Hence a natural question arises as to what happens if one deals with a system of $M>2$ parallel-coupled anharmonic chains. Is the wandering of the breather, initially excited at the edge (outermost) chain, across all chains possible? To study this problem, we start with a system of $M>2$ parallel weakly coupled anharmonic chains.

C. Simulation of breathers in a system of $M>2$ parallel weakly coupled anharmonic chains

The quasi-1D system of M parallel weakly coupled anharmonic chains, with nearest-neighbor intra- and interchain in-

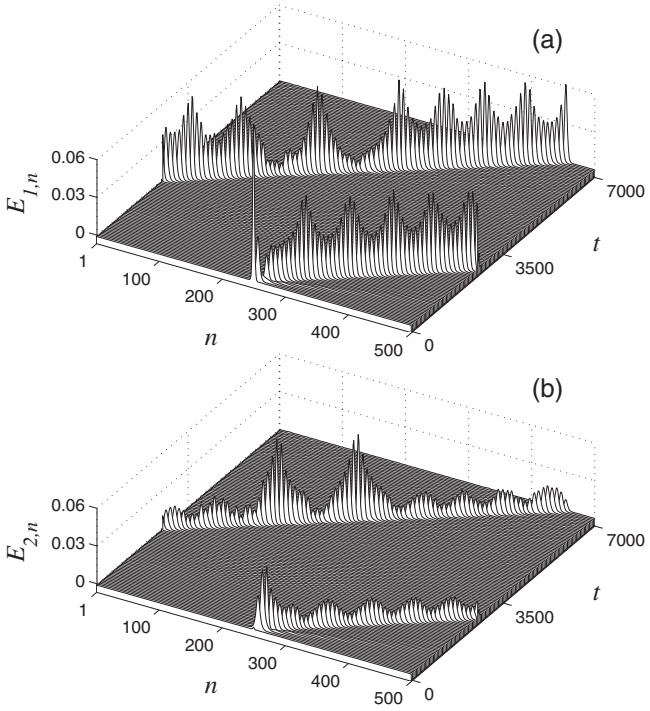

FIG. 11. Energy of a slowly moving wandering breather close to the separatrix in chain 1 (a) and chain 2 (b) versus time and site. The breather is initially excited in chain 1 with immovable chain 2, with velocity $V=0.1$ and amplitude $\Psi_{\max}=0.26$. The separatrix solution of Eq. (40) corresponds to $\Psi_{\max}=0.2582$. Separatrixlike dynamics, similar to the one shown in Fig. 7(b), is well established for $t \geq 4000$.

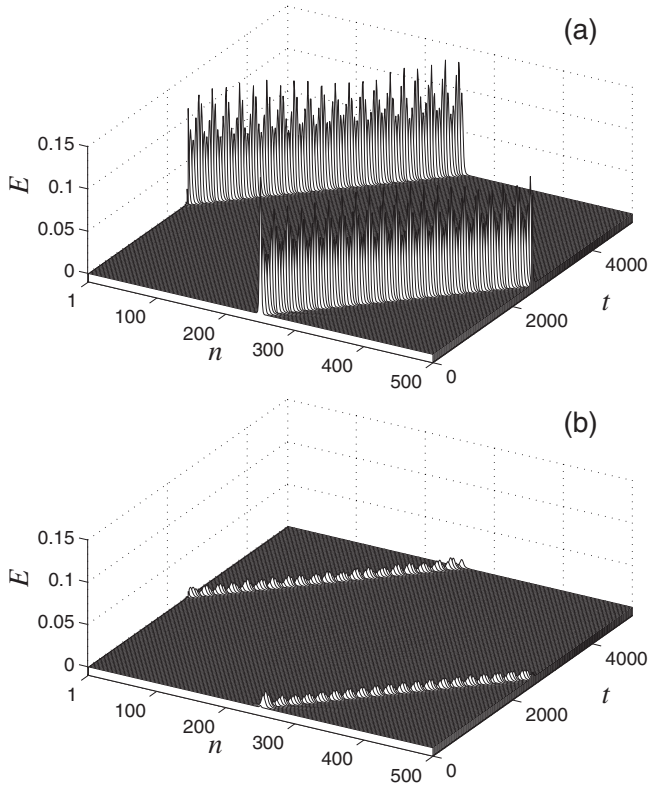

FIG. 12. Distribution of the breather energy in chain 1 (a) and chain 2 (b) versus time in the self-trapped regime of slowly moving breathers in two coupled chains with $C=0.1$, $\alpha=0$, and $\beta=1$. The breather was initially excited in chain 1 with immovable chain 2, with velocity $V=0.1$ and amplitude $\Psi_{\max}=0.3$.

teractions, is described by the following Hamiltonian:

$$H = \sum_{m=1}^{M} \sum_{n=1}^{N} \frac{1}{2} \dot{u}_{m,n}^2 + \sum_{m=1}^{M} \sum_{n=1}^{N-1} V(u_{m,n+1} - u_{m,n}) + \sum_{m=1}^{M-1} \sum_{n=1}^{N} U(u_{m+1,n} - u_{m,n}), \tag{60}$$

where $V(x)$ and $U(x)$ are given by Eqs. (51) and (52) and $n=1,\ldots,N$ and $m=1,\ldots,M$ numerate, respectively, sites along the chains and the chains.

The Hamiltonian (60) generates the corresponding equations of motion,

$$\ddot{u}_{m,n} = -\frac{\partial H}{\partial u_{m,n}}, \tag{61}$$

which in the linear approximation have the form

$$\ddot{u}_{m,n} = u_{m,n+1} - 2u_{m,n} + u_{m,n-1} + C(u_{m+1,n} - 2u_{m,n} + u_{m-1,n}). \tag{62}$$

Plane linear waves (phonons) in such a system, with

$$u_{m,n} = u \exp[iq_1 n + iq_2 m - i\omega t], \tag{63}$$

have the dispersion

$$\omega(q_1, q_2) = \sqrt{2[1 - \cos q_1 + C(1 - \cos q_2)]}, \tag{64}$$

where both the interchain spacing and intrachain lattice period are taken equal to unity, and therefore $0 \leq (q_1, q_2) \leq \pi$. The minimal phonon frequency in this translationally invariant system is zero, $\omega(0,0)=0$, while the cutoff phonon frequency is $\omega(\pi,\pi)=2\sqrt{1+C}$ [which is equal to $\omega(\pi,\pi)=2.0976 \approx 2.1$ for $C=0.1$].

Since we will be interested in the short-wavelength excitations, with $q_1 \approx \pi$, the corresponding phonon frequency for $C \ll 1$,

$$\omega(q_1 \approx \pi, q_2) = 2 + C \sin^2\left(\frac{1}{2} q_2\right), \tag{65}$$

determines the phonon group velocity across the chains:

$$V_\perp(q_1 \approx \pi, q_2) = \frac{\partial \omega(q_1 \approx \pi, q_2)}{\partial q_2} = \frac{1}{2} C \sin(q_2). \tag{66}$$

Now we turn to the nonlinear dynamics of M weakly coupled parallel nonlinear chains with Hamiltonian (60). We will integrate Eqs. (61) with the initial condition, which describes exact discrete breather in the mth chain ($1 \leq m \leq M$) under the condition of immovability of the rest of the chains, to study the time dependence (for $t>0$) of the vibration energy in the chains:

$$E_m = \frac{1}{2}\sum_{n=1}^{N} (\dot{u}_{m,n}^2 + V_{m,n} + V_{m,n-1} + U_{m,n} + U_{m-1,n}) \equiv \sum_{n=1}^{N} E_{n,m}, \tag{67}$$

where $V_{m,n}=V(u_{m,n+1}-u_{m,n})$, $U_{m,n}=U(u_{m+1,n}-u_{m,n})$, and breather energy $E=\Sigma_{m=1}^{M}E_m=\Sigma_{n=1}^{N}\Sigma_{m=1}^{M}E_{n,m}$.

By measuring the time dependence of $E_{n,m}$, we can define the breather center location (n_c,m_c),

$$n_c = \sum_{m=1}^{M}\sum_{n=1}^{N} np_{n,m}, \quad m_c = \sum_{m=1}^{M}\sum_{n=1}^{N} mp_{n,m}, \tag{68}$$

where $p_{n,m}=E_{n,m}/E$ describes the distribution of the normalized breather energy in a 2D lattice. With these breather quantities we can measure the longitudinal D_x (along the chain axis) and transverse D_y breather diameters:

$$D_x = 2\left[\sum_{m=1}^{M}\sum_{n=1}^{N} (n-n_c)^2 p_{n,m}\right]^{1/2},$$

$$D_y = 2\left[\sum_{m=1}^{M}\sum_{n=1}^{N} (m-m_c)^2 p_{n,m}\right]^{1/2}. \tag{69}$$

In Figs. 13(a)–13(d) we show the time dependence of energies of the first, $i=1$, and the last, $i=M$, coupled chains for $M=2,3,4,5$ for the time interval just after breather excitation in the first chain, left panels, and for the later time, right panels. In the case of $M=2$, there is a periodic and harmonic complete energy exchange between the first and second chains; see Fig. 13(a). In the case of $M=3$, there is periodic (and nonharmonic) recurrence of the complete energy accumulation in the first chain and the period of such recovery is twice larger (the recurrence rate is twice smaller) than that in the case of $M=2$. For $M=3$, the time dependence of the first chain energy recurrence can be roughly approximated as $\cos^4(Ct/8)$ [instead of $\cos^2\Theta=\cos^2(Ct/4)$ for $M=2$, Eqs. (19) and (45)], similar to the time dependence of the population of the initially excited state in a three-state (spin-1) atomic system; see, e.g., Ref. [57]. Here $C/4$ plays role of the Rabi frequency, which is twice smaller than the rate of the complete energy exchange (energy recurrence) in the case of $M=2$, when it is equal to $C/2$; see Eq. (45). In the case of $M=4$ and $M=5$, the recurrence of energy of the first and last chains becomes quasiperiodic [see Figs. 13(c) and 13(d)], but still the (approximate) period T_M of such recurrence scales with the number of chains M as $T_M \propto (M-1)$. For $M\geq 6$, $C=0.1$, the initially localized in chain-1 excitation spreads its energy in the whole system of weakly coupled chains.

The dependence of the recurrence period T_M on M we can relate with the transverse group velocity, Eq. (66), of the high-frequency phonons (with $q_1\approx\pi$) in the system of weakly linearly coupled anharmonic chains. The transverse wave vector q_2 in Eq. (66) is equivalent to the relative phase of the neighboring chains. In the regime of almost-harmonic energy transfer between the neighboring chains, the relative phase is always close to $\pi/2$; see Fig. 1. It means that the transverse wave vector q_2 in the expression (66) for the transverse group velocity of the wandering breather should also be (approximately) equal to $\pi/2$. In the case of the 2D system of coupled oscillator chains, $q_2=\pi/2$ corresponds to the case when, say, only the odd chains are excited at a given moment while their nearest neighbors, even chains, are at rest. This gives $V_\perp \approx \frac{1}{2}C$ for the transverse group velocity. Importantly, this characteristic group velocity does not depend on the number of the coupled chains, M. Therefore we can estimate the period of the first chain energy recovery as $T_M=2A(M-1)/V_\perp \approx 4A(M-1)/C$ with some dimensionless factor A, which is consistent with our numerical observation (with $A\approx 3$).

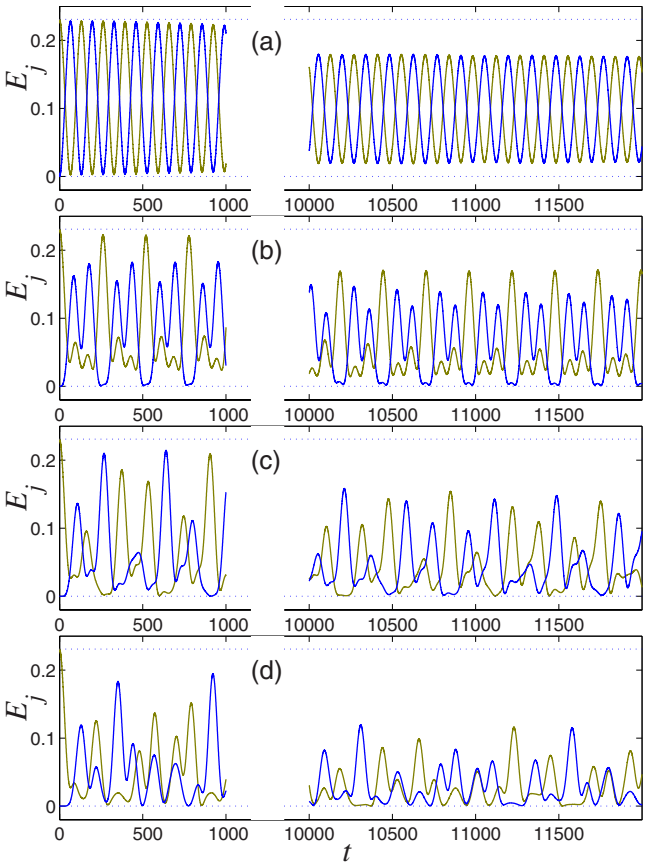

FIG. 13. (Color online) Time dependence of the breather energy in the first (green, light gray) and last (blue, dark gray) chains in a system of two (a), three (b), four (c), and five (d) chains with $C=0.1$, $\alpha=0$, and $\beta=1$. The breather is always initially excited with frequency $\omega=2.05$ in chain 1, with immovable rest of the chains.

The same transverse phonon group velocity one can estimate from Fig. 14 as the speed of breather spreading across the chains. Figure 14 shows the time dependence of energy distribution among the chains when the breather is initially excited in the edge chain, Figs. 14(a) and 14(b), or in the central chain, Figs. 14(c) and 14(d), in the system of $M=50$ coupled chains with $N=50$. As follows from Figs. 14(a) and 14(c), the initial breather energy spreads for 20 chains for approximately 500 time units. This gives us a quantitative estimate of 0.04 for the transverse group velocity, which is rather close to our analytical estimate with the use of Eq. (66) for $q_2\approx\pi/2$: $V_\perp \approx \frac{1}{2}C=0.05$. Figure 14 also shows that the appearance of localized breathers in a system of coupled

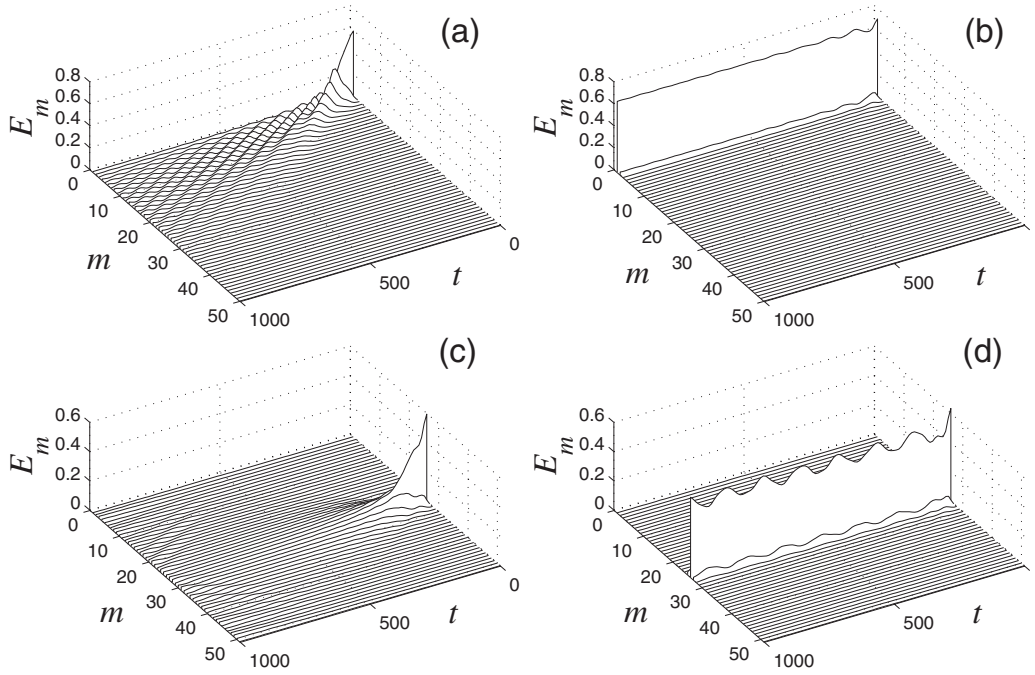

FIG. 14. Time dependence of the breather energy distribution between chains in a system of 50 coupled chains with $C=0.1$, $\alpha=0$, and $\beta=1$. Here m is the chain number and E_m is energy of the mth chain. The breather was initially excited with frequency $\omega=2.14$ in chain 1 (a), with frequency $\omega=2.15$ in chain 1 (b), with frequency $\omega=2.16$ in chain 25 (c), and with frequency $\omega=2.17$ in chain 25 (d), with immovable rest of chains.

chains, with $M \gg 2$, has a threshold in breather frequency, $\omega_{thresh}=2.15$ in Fig. 14(b) and $\omega_{thresh}=2.17$ in Fig. 14(d), similar to the case of two coupled chains. The threshold breather frequency, which corresponds to the appearance of localized breathers in a system of coupled chains, we should compare with the breather frequency at the separatrix in a system of two coupled chains, $\omega_{sep} \approx 2.1$; see Eq. (48) for $C=0.1$, $\alpha=0$, and $k=0$ and Figs. 7(b) and 7(c). Since all of the above frequencies are close, we can get an estimate for the threshold breather amplitude for its localization in the 2D system of weakly coupled chains: $\Psi_{\max}^{thresh} \sim \sqrt{C/\beta}$. For $\Psi_{\max} < \Psi_{\max}^{thresh}$, the 1D breather, which was initially excited in one chain, will start to translate laterally to the neighboring chains, will spread its energy among them and lose it due to phonon emission, and finally will decay into small-amplitude phonons due to a lowering of its frequency up to the cutoff phonon frequency $\omega_{\max}=2\sqrt{1+C}$; see Figs. 14(a) and 14(c). Such an evolution of low-amplitude 1D breathers can also be related to the above-mentioned conclusion that the wandering breather is not an exact solution of the nonlinear system even in the case of two coupled anharmonic chains. In contrast to such behavior of low-amplitude breathers, the 1D breather with amplitude $\Psi_{\max} > \Psi_{\max}^{thresh}$ is self-trapped and remains localized mainly in the chain of its initial excitation; see Figs. 14(b) and 14(d). [In Fig. 14(d) one can also see a partial (incomplete) energy exchange between the central chain and its nearest neighboring chains, similar to the incomplete energy exchange in two coupled chains beyond the separatrix; cf. Figs. 7(d).] This phenomenon resembles the so-called *delocalizing transition* in 2D systems, when the wave field abruptly changes its character from spatially localized to the extended one; cf. the similar delocalizing transition for polarons in 2D and 3D lattices [36] and for Bose-Einstein condensates in 2D optical lattices [37]. In our case, the delocalizing transition occurs by a decrease of the initial breather amplitude $\Psi_{\max}$ (or frequency ω) from the value $\Psi_{\max} > \Psi_{\max}^{thresh} \sim \sqrt{C/\beta}$ (or $\omega > \omega_{thresh}$) to the value $\Psi_{\max} < \Psi_{\max}^{thresh}$ (or $\omega < \omega_{thresh}$). Such a transition is related to the finite energy threshold for the creation of solitons and breathers in 2D and 3D systems (see Refs. [58,59]) and is absent in 1D (β-FPU or discrete nonlinear Schrödinger equation [36,37]) systems. Indeed, the threshold breather amplitude $\Psi_{\max}^{thresh}$ in strongly anisotropic quasi-1D systems vanishes in the limit $C \to 0$ of a single 1D chain since $\Psi_{\max}^{thresh} \sim \sqrt{C/\beta}$. A similar threshold breather amplitude $\Psi_{\max}^{thresh} \sim \sqrt{C/\beta}$ for breather delocalization should also appear in 3D arrays of parallel weakly coupled nonlinear chains, with coupling constant $C \ll 1$, which are described by the FPU Hamiltonian, similar to the one given by Eq. (1).

To get deeper insight into the delocalizing transition of the discrete breather in 2D systems of weakly coupled chains, we confirm numerically that the discrete breather in 2D systems of weakly coupled chains is stable only in the frequency range $[\omega_b, \infty)$, where $\omega_b=2.12$ for $C=0.1$ is higher than the cutoff phonon frequency $\omega(\pi,\pi)=2\sqrt{1+C} \approx 2.1$. This means that there is a frequency gap $[\omega(\pi,\pi), \omega_b]$ above the cutoff phonon frequency in which there are no solutions for localized breathers in 2D systems: breathers with frequencies in the gap spread across all 2D lattices. The frequency ω_b is close to the threshold frequencies ω_{thresh} aforementioned and indicated in Fig. 14, but the frequency ω_b does not depend on the breather excitation in 2D lattices, in contrast to the threshold frequencies. In Fig. 15 we plot the breather energy distributions along and across the chains for

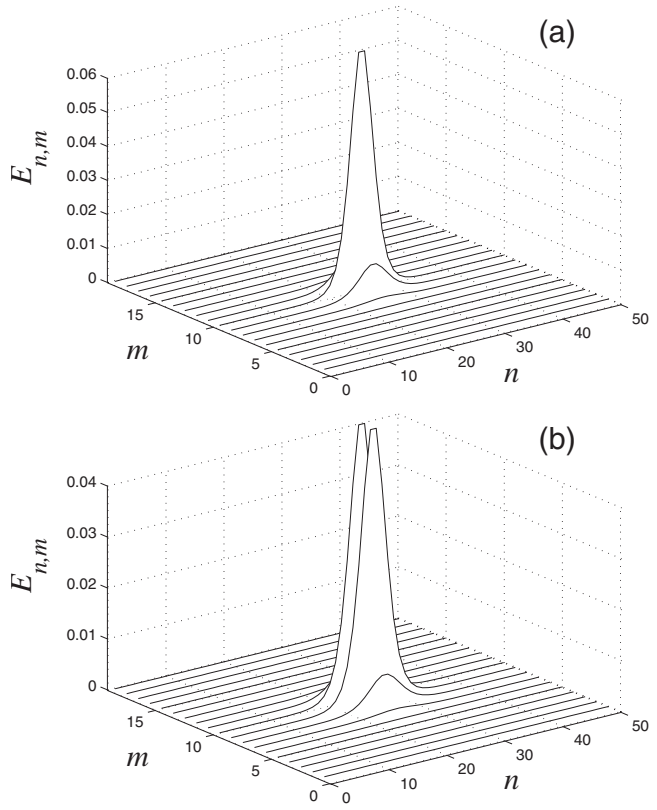

FIG. 15. Distribution of the vibration energy in a 2D lattice of weakly coupled nonlinear chains, with $\alpha=0$, $\beta=1$, and $C=0.1$, along (n) and across (m) the chains for a one-chain (a) and antiphase two-chain (b) breather with frequency $\omega=2.12$.

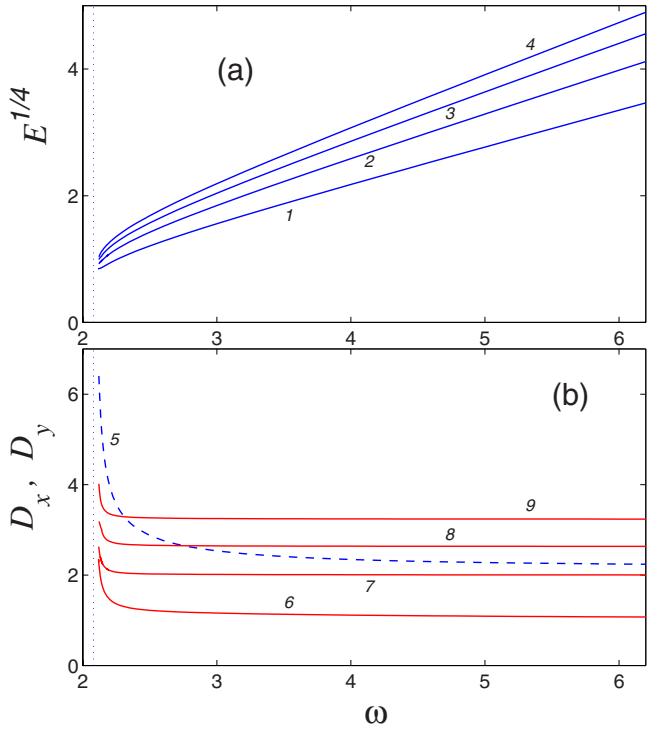

FIG. 16. (Color online) Dependence of the breather vibrational energy (a) and longitudinal D_x and transverse D_y breather diameters (b) versus breather frequency for one-chain (curves 1, 5, and 6), antiphase two-chain (curves 2, 5, and 7), antiphase three-chain (curves 3, 5, and 8), and antiphase four-chain (curves 4, 5, and 9) breathers in a multichain system ($M=20$, $N=50$). The dashed line corresponds to the longitudinal breather diameter. The vertical dotted line shows the cutoff phonon frequency.

the one-chain, Fig. 15(a), and antisymmetric (antiphase) two-chain, Fig. 15(b), breathers in a 2D lattice with $\omega=\omega_b=2.12$, which show that the transverse localization length of the discrete breather has the order of the interchain spacing for $\omega=\omega_b$ [and further decreases for $\omega>\omega_b$; see Fig. 16(b) below].

In addition to the one- and two-chain breathers, there are also three-chain, four-chain, etc., in-phase and antiphase breathers in a multichain system. In Fig. 16 we show the breather vibrational energy and the measured [with the use of Eqs. (67)–(69)] longitudinal and transverse breather diameters for the one-, two-, three-, and four-chain antiphase breathers. As one can see from this figure, the breather energy grows as ω^4 in the high-energy limit. This dependence can easily be understood from Eqs. (16) and (22) for breather energy E_b and frequency ω: one has $E_b \propto \Psi_{\max}^4$ and $\omega \propto \Psi_{\max}$ in the large-amplitude limit; see also Ref. [22]. The breather with threshold frequency $\omega=\omega_b$ has minimal energy: $E_b=0.517$ and $E_b=0.740$ for the one- and antiphase two-chain breathers, respectively. From Fig. 16(b) we can also see that, in accordance with Fig. 15(a), the transverse localization length of the one-chain breather at the threshold frequency is very close to the interchain spacing and further decreases with the increase of breather energy. [Both longitudinal and transverse breather diameters saturate at the amplitude-independent values in the high-energy limit (see, e.g., [7]), when the transverse diameter of the m-chain breather is simply $D_y \approx B(m+1)$ with $B \cong 1$; see Fig. 16(b).] This means that there are no laterally localized envelope-soliton vibrational excitations in our 2D system of parallel-coupled nonlinear oscillator chains, in contrast to the laterally localized envelope-soliton optical excitations in 2D arrays of parallel-coupled nonlinear optical waveguides [11]. Therefore the interchain breather translation and wandering are possible only in a system of small number of coupled oscillator chains ($M \leq 5$ for $C=0.1$), while in a multichain 2D system ($M \geq 6$ for $C=0.1$) the vibrational breathers can move only along the chains. Such 1D motion of 1D breathers in a 2D system of multiple parallel weakly coupled oscillator chains resembles the 1D motion of 1D interacting Bose gases in a 2D array of multiple parallel weakly coupled atom waveguides (a quantum Newton's cradle) [28] (see also [60]).

IV. SUMMARY

In summary, we have found, both analytically and numerically, two qualitatively different regimes of energy exchange between phase-coherent breathers (intrinsically localized short-wave nonlinear excitations) in two weakly coupled nonlinear oscillator chains. In the low-amplitude mode, the breather performs periodic transverse translations (wandering) between the coupled chains. In the large-amplitude mode, the breather is self-trapped in one chain.

These two breather modes are detached by a separatrix, at which the rate of the interchain energy exchange vanishes. These two regimes have a profound analogy—and are described by a similar pair of equations—to the Josephson plasma oscillations and nonlinear self-trapping, recently observed in a single-bosonic Josephson junction [31]. The predicted evolution of the relative phase of two weakly coupled coherent breathers in both regimes is also analogous to the evolution of relative quantum-mechanical phase between two weakly coupled macroscopic Bose-Einstein condensates, which was directly measured in a single-bosonic Josephson junction by means of interference [31]. On the basis of this profound analogy, we predict a tunneling regime of two weakly linked Bose-Einstein condensates in which their relative phase oscillates around $\frac{\pi}{2}$ mod π, which can be observed by means of interference. The similarity between the classical phase-coherent excitation exchange and macroscopic tunneling quantum dynamics found here can encourage new experiments in both fields.

We also show that the magnitude of the static displacements of the coupled chains with nonlinear localized excitation, induced by cubic term in the intrachain anharmonic potential, scales approximately as the total vibrational energy of the excitation, either one- or two-chain one, and does not depend on the interchain coupling. This feature is also valid for a narrow stripe of several parallel-coupled nonlinear chains. We also study two-chain breathers, which can be considered as bound states of discrete breathers with different symmetry and center locations in the coupled chains, and bifurcation of the antiphase two-chain breather into the one-chain one. Bound states of two breathers with different commensurate frequencies are found in the two-chain system. Merging of two breathers with different frequencies in one breather in two coupled chains is observed. Wandering of the low-amplitude breather in a system of several, up to five, coupled nonlinear chains is studied, and the dependence of the wandering period on the number of chains is analytically estimated and compared with numerical results.

Delocalizing transition of a 1D breather in a 2D system of a large number of parallel-coupled nonlinear chains is described, in which the breather, initially excited in a given chain, abruptly spreads its vibrational energy in the whole 2D system upon decreasing breather frequency or amplitude below the threshold one. The threshold breather frequency is above the cutoff phonon frequency in the 2D system, the threshold breather amplitude scales as the square root of the interchain coupling constant, and the breather vibrational energy is localized mainly in one chain at the delocalization threshold. A similar delocalizing transition for 1D breathers should also occur in 3D arrays of parallel-coupled nonlinear oscillator chains. The delocalizing transition of discrete vibrational breathers in 2D and 3D systems of coupled nonlinear oscillator chains has an analogy with the delocalizing transition for Bose-Einstein condensates in 2D and 3D optical lattices.

ACKNOWLEDGMENTS

Yu.A.K. is grateful to S. Aubry, E. Bogomolny, S. Flach, V. Fleurov, A. S. Kovalev, and G. Shlyapnikov for useful discussions. This work was supported by the Presidium of the Russian Academy of Sciences (Grant No. 04/BGTCh-07) and Russian Foundation for Basic Research (Grant No. 05-03-32241).

[1] N. J. Zabusky and M. D. Kruskal, Phys. Rev. Lett. **15**, 240 (1965).
[2] A. M. Kosevich and A. S. Kovalev, Zh. Eksp. Teor. Fiz. **67**, 1793 (1974) [Sov. Phys. JETP **40**, 891 (1974)].
[3] A. S. Dolgov, Fiz. Tverd. Tela (Leningrad) **28**, 1641 (1986) [Sov. Phys. Solid State **28**, 907 (1986)].
[4] A. J. Sievers and S. Takeno, Phys. Rev. Lett. **61**, 970 (1988).
[5] J. B. Page, Phys. Rev. B **41**, 7835 (1990).
[6] Yu. A. Kosevich, Phys. Lett. A **173**, 257 (1993); Phys. Rev. B **47**, 3138 (1993); **48**, 3580(E) (1993).
[7] Yu. A. Kosevich, Phys. Rev. Lett. **71**, 2058 (1993).
[8] A. J. Sievers and J. B. Page, in *Dynamical Properties of Solids*, edited by G. K. Horton and A. A. Maradudin (North-Holland, Amsterdam, 1995), Vol. 7, p. 131.
[9] S. Aubry, Physica D **103**, 201 (1997); **216**, 1 (2006).
[10] S. Flach and C. R. Willis, Phys. Rep. **295**, 181 (1998).
[11] H. S. Eisenberg, Y. Silberberg, R. Morandotti, A. R. Boyd, and J. S. Aitchison, Phys. Rev. Lett. **81**, 3383 (1998).
[12] J. W. Fleischer, M. Segev, N. K. Efremidis, and D. N. Christodoulides, Nature (London) **422**, 147 (2003).
[13] B. I. Swanson, J. A. Brozik, S. P. Love, G. F. Strouse, A. P. Shreve, A. R. Bishop, W.-Z. Wang, and M. I. Salkola, Phys. Rev. Lett. **82**, 3288 (1999).
[14] M. Sato and A. J. Sievers, Nature (London) **432**, 486 (2004).
[15] E. Trias, J. J. Mazo, and T. P. Orlando, Phys. Rev. Lett. **84**, 741 (2000).
[16] P. Binder, D. Abraimov, A. V. Ustinov, S. Flach, and Y. Zolotaryuk, Phys. Rev. Lett. **84**, 745 (2000).
[17] D. K. Campbell, S. Flach, and Y. S. Kivshar, Phys. Today **57** (1), 43 (2004).
[18] J. Edler, R. Pfister, V. Pouthier, C. Falvo, and P. Hamm, Phys. Rev. Lett. **93**, 106405 (2004).
[19] M. E. Manley, M. Yethiraj, H. Sinn, H. M. Volz, A. Alatas, J. C. Lashley, W. L. Hults, G. H. Lander, and J. L. Smith, Phys. Rev. Lett. **96**, 125501 (2006).
[20] D. Chen, S. Aubry, and G. P. Tsironis, Phys. Rev. Lett. **77**, 4776 (1996).
[21] Yu. A. Kosevich and S. Lepri, Phys. Rev. B **61**, 299 (2000).
[22] Yu. A. Kosevich and G. Corso, Physica D **170**, 1 (2002).
[23] Yu. A. Kosevich, R. Khomeriki, and S. Ruffo, Europhys. Lett. **66**, 21 (2004).
[24] L. V. Yakushevich, A. V. Savin, and L. I. Manevitch, Phys. Rev. E **66**, 016614 (2002).
[25] A. V. Savin and L. I. Manevitch, Phys. Rev. B **67**, 144302 (2003).
[26] A. V. Savin, E. A. Zubova, and L. I. Manevitch, Phys. Rev. B

71, 224303 (2005).
[27] B. P. Anderson and M. A. Kasevich, Science **282**, 1686 (1998).
[28] T. Kinoshita, T. Wenger, and D. S. Weiss, Nature (London) **440**, 900 (2006).
[29] G. J. Milburn, J. Corney, E. M. Wright, and D. F. Walls, Phys. Rev. A **55**, 4318 (1997).
[30] Yu. A. Kosevich, L. I. Manevitch, and A. V. Savin, J. Phys.: Conf. Ser. **92**, 012093 (2007).
[31] M. Albiez, R. Gati, J. Fölling, S. Hunsmann, M. Cristiani, and M. K. Oberthaler, Phys. Rev. Lett. **95**, 010402 (2005).
[32] A. Smerzi, S. Fantoni, S. Giovanazzi, and S. R. Shenoy, Phys. Rev. Lett. **79**, 4950 (1997).
[33] S. Raghavan, A. Smerzi, S. Fantoni, and S. R. Shenoy, Phys. Rev. A **59**, 620 (1999).
[34] M. Greiner, O. Mandel, T. Esslinger, Th. Hänsch, and I. Bloch, Nature (London) **415**, 39 (2002).
[35] R. Gati, B. Hemmerling, J. Fölling, M. Albiez, and M. K. Oberthaler, Phys. Rev. Lett. **96**, 130404 (2006).
[36] G. Kalosakas, S. Aubry, and G. P. Tsironis, Phys. Rev. B **58**, 3094 (1998).
[37] G. Kalosakas, K. O. Rasmussen, and A. R. Bishop, Phys. Rev. Lett. **89**, 030402 (2002).
[38] For a review, see Chaos **15** (1) (2005).
[39] S. R. Bickham, S. A. Kiselev, and A. J. Sievers, Phys. Rev. B **47**, 14206 (1993).
[40] G. Huang, Z. Shi, and Z. Xu, Phys. Rev. B **47**, 14561 (1993).
[41] S. A. Kiselev, S. R. Bickham, and A. J. Sievers, Phys. Rev. B **48**, 13508 (1993).
[42] A. A. Ovchinnikov, Zh. Eksp. Teor. Fiz. **57**, 263 (1969) [Sov. Phys. JETP **30**, 147 (1970)].
[43] S. M. Jensen, IEEE J. Quantum Electron. **18**, 1580 (1982).
[44] A. M. Kosevich and A. S. Kovalev, *Introduction to Nonlinear Physical Mechanics* (Naukova Dumka, Kiev, 1989) (in Russian).
[45] G. P. Tsironis, Phys. Lett. A **173**, 381 (1993).
[46] M. F. Jorgensen and P. L. Christiansen, Chaos, Solitons Fractals **4**, 217 (1994).
[47] A. I. Manevich and L. I. Manevitch, *The Mechanics of Nonlinear Systems with Internal Resonances* (Imperial College Press, London, 2005).
[48] A. J. Lichtenberg and M. A. Liberman, *Regular and Chaotic Dynamics* (Springer-Verlag, New York, 1992).
[49] Yu. A. Kosevich, Phys. Rev. B **63**, 205313 (2001).
[50] N. Akhmediev and A. Ankiewicz, Phys. Rev. Lett. **70**, 2395 (1993).
[51] I. M. Uzunov, R. Muschall, M. Gölles, Y. S. Kivshar, B. A. Malomed, and F. Lederer, Phys. Rev. E **51**, 2527 (1995).
[52] Th. P. Valkering, J. van Honschoten, and H. J. W. M. Hoekstra, Opt. Commun. **159**, 215 (1999).
[53] J. C. Eilbeck, P. S. Lomdahl, and A. C. Scott, Physica D **16**, 318 (1985).
[54] S. Aubry, S. Flach, K. Kladko, and E. Olbrich, Phys. Rev. Lett. **76**, 1607 (1996).
[55] M. Kastner, Phys. Rev. Lett. **92**, 104301 (2004).
[56] Ying-Ju Wang, D. Z. Anderson, V. M. Bright, E. A. Cornell, Q. Diot, T. Kishimoto, M. Prentiss, R. A. Saravanan, S. R. Segal, and S. Wu, Phys. Rev. Lett. **94**, 090405 (2005).
[57] M.-O. Mewes, M. R. Andrews, D. M. Kurn, D. S. Durfee, C. G. Townsend, and W. Ketterle, Phys. Rev. Lett. **78**, 582 (1997).
[58] A. S. Kingsep, L. I. Rudakov, and R. N. Sudan, Phys. Rev. Lett. **31**, 1482 (1973).
[59] S. Flach, K. Kladko, and R. S. MacKay, Phys. Rev. Lett. **78**, 1207 (1997).
[60] K. Winkler, G. Thalhammer, F. Lang, R. Grimm, J. Hecker Denschlag, A. J. Daley, A. Kantian, H. P. Büchler, and P. Zoller, Nature (London) **441**, 853 (2006).